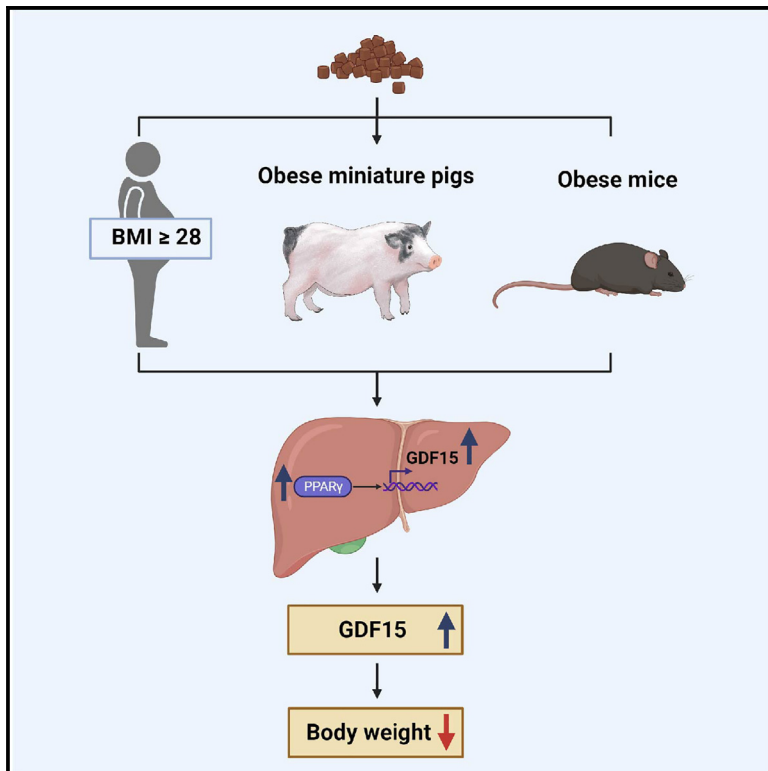


Cell Metabolism

GDF15 is a major determinant of ketogenic diet-induced weight loss

Graphical abstract



Authors

Jun Feng Lu, Meng Qing Zhu, Bo Xia, ..., Ying Qi Zhang, Xiao Miao Li, Jiang Wei Wu

Correspondence

xiaomiao@fmmu.edu.cn (X.M.L.), wujiangwei@nwafu.edu.cn (J.W.W.)

In brief

Application of a ketogenic diet (KD) for obesity management has been widely promoted, yet its underlying mechanism remains elusive. Here Lu et al. reveal a major role for GDF15 in this process. Their findings uncover a liver PPAR γ -GDF15-dependent mechanism underlying KD-mediated obesity management, advancing the understanding of KD's metabolic actions.

Highlights

- KD feeding reduces body weight and increases circulating GDF15 levels
- GDF15-GFRAL signaling pathway is required for KD-mediated weight loss
- Hepatic PPAR γ regulates the transcription and production of GDF15 in KD-fed mice
- GDF15 administration restores abolished weight loss effect of KD in *Ppar γ ^{Δ Hep}* mice



Article

GDF15 is a major determinant of ketogenic diet-induced weight loss

Jun Feng Lu,^{1,5} Meng Qing Zhu,^{1,5} Bo Xia,^{1,5} Na Na Zhang,^{2,5} Xiao Peng Liu,¹ Huan Liu,¹ Rui Xin Zhang,¹ Jun Ying Xiao,¹ Hui Yang,³ Ying Qi Zhang,⁴ Xiao Miao Li,^{2,*} and Jiang Wei Wu^{1,6,*}

¹Key Laboratory of Animal Genetics, Breeding and Reproduction of Shaanxi Province, College of Animal Science and Technology, Northwest A&F University, Yangling, Shaanxi 712100, China

²Department of Endocrinology and Metabolism, First Affiliated Hospital of Air Force Medical University, Xi'an, Shaanxi 710032, China

³National Health Commission (NHC) Key Laboratory of Food Safety Risk Assessment, China National Center for Food Safety Risk Assessment, Beijing 100022, China

⁴State Key Laboratory of Cancer Biology, Biotechnology Center, School of Pharmacy, Air Force Medical University, Xi'an, Shaanxi 710032, China

⁵These authors contributed equally

⁶Lead contact

*Correspondence: xiaomiao@fmmu.edu.cn (X.M.L.), wujiangwei@nwafu.edu.cn (J.W.W.)

<https://doi.org/10.1016/j.cmet.2023.11.003>

SUMMARY

A ketogenic diet (KD) has been promoted as an obesity management diet, yet its underlying mechanism remains elusive. Here we show that KD reduces energy intake and body weight in humans, pigs, and mice, accompanied by elevated circulating growth differentiation factor 15 (GDF15). In GDF15- or its receptor GFRAL-deficient mice, these effects of KD disappeared, demonstrating an essential role of GDF15-GFRAL signaling in KD-mediated weight loss. *Gdf15* mRNA level increases in hepatocytes upon KD feeding, and knockdown of *Gdf15* by AAV8 abrogated the obesity management effect of KD in mice, corroborating a hepatic origin of GDF15 production. We show that KD activates hepatic PPAR γ , which directly binds to the regulatory region of *Gdf15*, increasing its transcription and production. Hepatic *Ppar γ* -knockout mice show low levels of plasma GDF15 and significantly diminished obesity management effects of KD, which could be restored by either hepatic *Gdf15* overexpression or recombinant GDF15 administration. Collectively, our study reveals a previously unexplored GDF15-dependent mechanism underlying KD-mediated obesity management.

INTRODUCTION

The obesity epidemic contributes to the increased health burden of metabolic diseases, cardiovascular disease, and even cancer, affecting more than 900 million people worldwide.^{1,2} Therefore, it is a great threat to human health and a heavy burden on public health systems. Due to unsatisfactory results of interventions on physical activity and the safety of anti-obesity drugs, dietary modification has been proposed as an effective strategy and a cornerstone for obesity management.^{3,4} In the past several decades, a plethora of efforts have been devoted to exploring obesity management diets such as macronutrient composition at various carbohydrate, protein, and fat levels, as well as calorie restrictions such as intermittent fasting.³ However, there is not a one-size-fits-all diet for obesity management. It is important to tailor dietary recommendations and optimize adherence for the individual. The ketogenic diet (KD), a high-fat, adequate-protein, and very-low-carbohydrate (or no carbohydrate) diet,⁵ has emerged as an alternative option for obesity management.^{6,7}

KD has been established as a successful dietary approach for the treatment of intractable epilepsy and has garnered research attention rapidly in the past decade.^{5,8} It increases circulating ketone bodies, which can be used as an alternative energy source to glucose.⁹ This state of “metabolic ketosis” is similar to a fasting state. Thus, KD is a compromise to fasting. In mice, KD has been shown to reduce blood glucose, increase insulin sensitivity, and even enhance longevity and “health span.”^{10,11} In humans, KD has been used to reduce seizures in patients with epilepsy since the 1970s.^{8,12} Currently, KD is under evaluation for polycystic ovarian syndrome, polycystic kidney disease, chronic pain, neurodegenerative diseases, influenza virus infection, tumor growth, and cancer,^{13–18} as well as being a nutrition approach for regular individuals or trained athletes.^{5,19} Among these versatile functions, the beneficial effects of KD on obesity management have attracted a significant amount of attention and many followers,^{20,21} while its underlying mechanism remains elusive.

Growth differentiation factor 15 (GDF15) is a distinct member of the transforming growth factor β (TGF- β) superfamily and



MS1

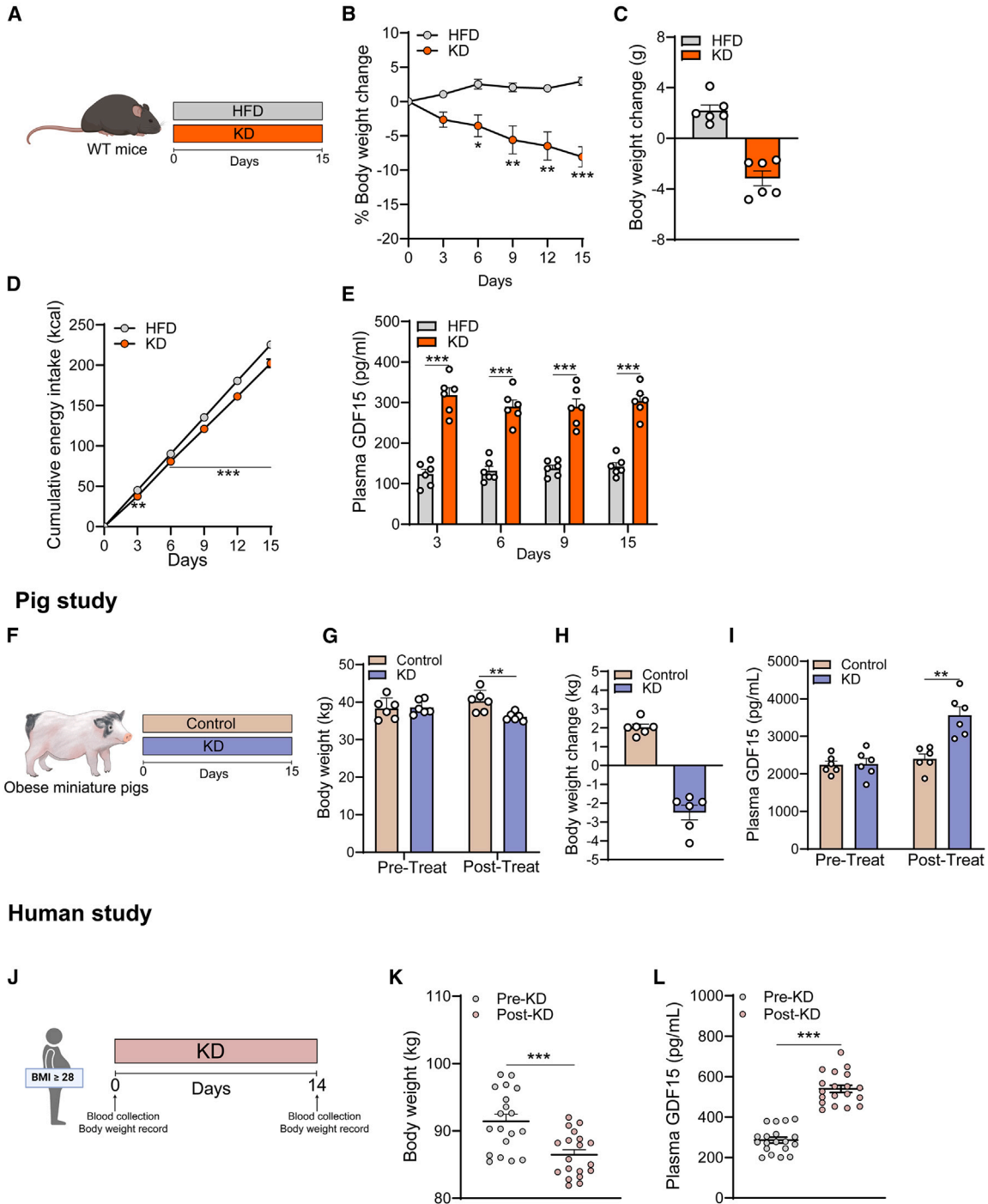


Figure 1. KD feeding reduces body weight accompanied by elevated circulating GDF15

(A–E) Mouse study 1 (MS1).

(A) Schematic diagram of mouse feeding.

(B and C) Body weight changes.

(D) Cumulative energy intake (kcal).

(E) Plasma levels of GDF15 at indicated time points. Data points show individual mice. Six mice per group.

(F–I) Pig study.

(F) Schematic diagram of pig feeding.

(G) Body weight.

(legend continued on next page)

was first characterized in the late 1990s by several labs.^{22–24} Circulating levels of GDF15 have been reported to be markedly elevated in humans in a broad spectrum of cellular stress (e.g., obesity, cardiac and renal failure, chronic liver disease, and various cancers)^{25,26} and mitochondrial diseases,^{27,28} where it is widely considered to be a useful biomarker.^{29,30} GDF15 expression can be induced in a variety of tissues (e.g., liver, kidney, intestines, and placenta) in response to a variety of different stimuli.^{27,31,32} Transgenic overexpression or pharmacological administration of GDF15^{33–35} under obesogenic conditions improved metabolic parameters, promoting it as a new target for obesity prevention and treatment.^{36–38} Its cognate receptor GFRAL was identified simultaneously and independently in late 2017.^{35,39,40} These groundbreaking findings evoke enthusiasm to explore the regulation of GDF15 and its therapeutic application in obesity treatment.^{26,41–44} One characteristic feature of GDF15 is suppression of food intake.^{36,45} Several reports and our preliminary work repeatedly showed reduced food intake in KD-fed animals,^{46,47} suggesting a potential link between GDF15 and the obesity management of KD.

In this study, we investigated the role of GDF15 in KD-mediated weight loss and associated beneficial metabolic effects. KD feeding induces mild elevation of circulating GDF15, which suppresses energy intake and reduces body fat mass. Using either *Gdf15*^{-/-} or *Gfral*^{-/-} mice, we show that the GDF15-GFRAL axis is crucial for the weight-lowering effects of KD. We also corroborate that KD-induced GDF15 derives from activation of hepatic PPAR γ . The beneficial effects of KD on obesity management greatly diminished in hepatic *Ppar γ* -knockout mice, which could be markedly restored by an AAV-*Gdf15* or recombinant GDF15. Together, our findings reveal insight into the obesity management effects of KD.

RESULTS

KD feeding reduces body weight accompanied by elevated circulating GDF15 in mice, pigs, and humans

To understand KD-mediated weight management, we first fed obese mice a KD or a control high-fat diet (HFD) for 15 days (Figure 1A) and observed gradually decreased body weight in the KD group compared to the weight gain in the HFD group from the 6th day on. Fifteen-day KD feeding reduced the body weight of mice from 39.10 \pm 0.33 to 35.94 \pm 0.61 g (Figures 1B and 1C). We also noticed reduced cumulative energy intake (kcal) in the KD-fed mice starting from day 3 (16.48%) (Figure 1D), accompanied by an \sim 2-fold increase in circulating GDF15 (Figure 1E). To further determine whether KD-induced GDF15 is relatively specific, we measured circulating GDF15 in mice fed several widely used obesity management diets, including the Mediterranean diet,^{48,49} low-fat diet,⁵⁰ high-protein diet,⁵¹ and low-glycemic-index diet⁵² (Figures S1A

and S1B), as well as two fasting regimes: every-other-day fasting⁵³ and time-restricted feeding⁵⁴ (Figures S1C–S1F). The results showed that these types of diets were unable to elevate circulating GDF15 within the tested period of time in mice. In order to gain more confidence about the relationship between KD and GDF15, one of the widely used preclinical models, pig, was chosen for this dietary intervention trial (Figure 1F). We observed decreased body weight in the KD-fed pigs (Figures 1G and 1H) with an increase (\sim 1.5-fold) in circulating levels of GDF15 (Figure 1I) after 15 days of treatment. Finally, we recruited a cohort of participants with obesity for a 2-week KD intervention (Figures 1J and 1K). Reduced body weight (from 91.44 \pm 1.04 to 86.47 \pm 0.75 kg) and elevated circulating levels of GDF15 (\sim 1.9-fold) were shown in these individuals at the end of the intervention (Figure 1L). Together, these results suggest that KD feeding reduces body weight and increases circulating GDF15.

GDF15-GFRAL signaling is required for the weight-loss effects of KD

We next sought to investigate the role of GDF15 in obesity management of KD. To this end, *Gdf15*-deficient (*Gdf15*^{-/-}) mice were used and given a KD for 30 days. Consistent with the above short-term feeding, a 30-day KD treatment significantly increased circulating levels of GDF15 (2.26-fold) in wild-type (WT) mice, but not in *Gdf15*^{-/-} mice (Figure 2A). KD feeding reduced cumulative energy intake (Figure 2B) and body weight (Figure 2C) in WT mice, but not in *Gdf15*^{-/-} mice. Instead, KD feeding increased the body weight of *Gdf15*^{-/-} mice from 32.19 \pm 0.93 to 35.29 \pm 0.79 g (on day 1 versus day 30, $p < 0.001$), equivalent to a weight gain of 9.64% \pm 1.98% relative to their initial weights. The body weights of KD-fed *Gdf15*^{-/-} mice almost caught up with those of HFD controls (Figure 2C). Similarly, KD feeding reduced the fat mass and liver weight in WT mice, but not in the *Gdf15*^{-/-} group (Figures 2D and 2E). Consistent with body weight reduction, KD feeding reduced plasma levels of triglycerides (TGs) (Figure 2F), alanine aminotransferase (ALT) and aspartate aminotransferase (AST) (Figure 2G), and hepatic TG content (Figure 2H) and improved glucose tolerance (Figures 2I and 2J) as well as insulin sensitivity (Figures 2K–2L) in WT mice, whereas these beneficial effects were not shown in the absence of GDF15. Collectively, these results suggest that GDF15 is indispensable for KD-mediated obesity management in mice.

We further test whether elevation of circulating GDF15 contributes to the weight loss effects of KD by using a GDF15 neutralizing antibody. The efficiency of this antibody was validated in a cohort of WT mice received either exogenous GDF15 alone or along with coadministration of this antibody (Figures S2A and S2B). KD-consuming mice treated with IgG showed reduced body weight compared with their corresponding HFD controls,

(H) Body weight changes.

(I) Plasma levels of GDF15. Six pigs per group.

(J–L) Human study.

(J) Schematic diagram of human study.

(K and L) Body weight (K) and plasma levels (L) of GDF15 before and after KD intervention in participants with obesity. $n = 19$ individuals.

Data are presented as mean \pm SEM. * $p < 0.05$, ** $p < 0.01$, *** $p < 0.001$. HFD, high-fat diet; KD, ketogenic diet.

See also Figure S1.

MS2

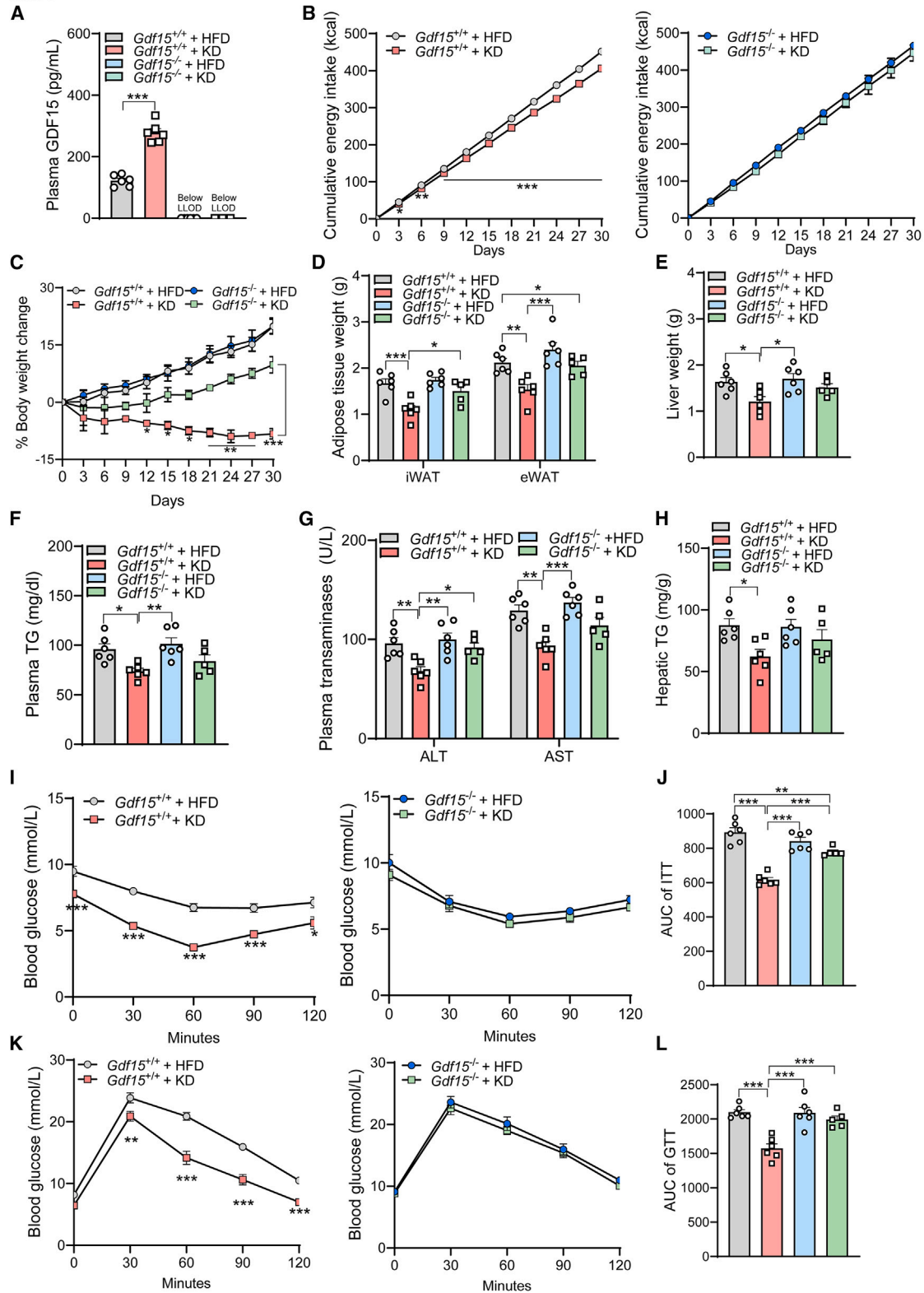


Figure 2. GDF15 is required for the weight-loss effects of KD

Mouse study 2 (MS2): WT and *Gdf15*^{-/-} mice were under HFD or KD feeding for 30 days.

(A) Plasma levels of GDF15 on day 18. LLOD, lower limit of detection.

(legend continued on next page)

whereas the weight loss seen in KD-fed mice was greatly diminished with anti-GDF15 treatment, reaching $4.32\% \pm 1.83\%$ above starting body weight (Figures S2C and S2D), suggesting that GDF15 directly mediates the weight loss effects of KD.

The role of GDF15 in KD-mediated weight control was also tested in *Gfral*^{-/-} mice. Despite elevated circulating GDF15 (Figure 3A), KD was unable to reduce cumulative energy intake (Figure 3B), body weight (Figure 3C), fat mass (Figure 3D), and liver weight (Figure 3E) in the absence of GFRAL. Also, the beneficial effects of KD on hepatic TGs (Figure 3F), plasma ALT and AST (Figure 3G), glucose tolerance (Figures 3H and 3I), and insulin sensitivity (Figures 3J and 3K) were not preserved in *Gfral*^{-/-} mice. Together, these results demonstrate that GDF15-GFRAL signaling plays an important role in the beneficial metabolic actions of KD in mice.

The anti-obesity effects of KD are achieved by orchestration of GDF15-mediated energy intake suppression and FGF21-conferred energy expenditure

To test whether reduced energy intake solely or along with altered energy expenditure contributes to the body weight control effect of KD in mice, we first applied a pair-feeding regime (by energy) to mice to investigate whether this could abrogate the weight difference between KD-fed mice and HFD controls (Figure S3A). Pair-feeding largely but not completely abolished the weight difference between KD and HFD mice (Figure S3B), suggesting (1) a major role of energy intake suppression in this process and (2) a potential contribution of energy expenditure. We then undertook the indirect calorimetry in *Gdf15*^{-/-} and WT mice fed KD and HFD under *ad libitum* conditions to establish whether there are additional effects on energy expenditure. KD-fed mice showed higher energy expenditure than HFD controls irrespective of GDF15 when data were analyzed by analysis of covariance (ANCOVA) with body lean mass as the covariate (Figures S3C and S3D). These results, together with the above GDF15-dependent suppression of energy intake under KD conditions (Figures 2B and 2C), suggest that KD-mediated obesity management involves GDF15-regulated energy intake as well as GDF15-independent energy expenditure.

KD feeding is reported to increase circulating FGF21,⁵⁵ a hormone known to increase energy expenditure.^{56–58} We thus measured circulating FGF21 and found increased levels in KD-fed WT and *Gdf15*^{-/-} mice, as well as elevated *Fgf21* mRNA in their livers (Figures S4A and S4B). To explore whether the increased GDF15-independent energy expenditure under KD feeding is due to FGF21, we treated KD-fed *Gdf15*^{-/-} mice and WT controls with an FGF21 neutralizing antibody (Fig-

ure S4C) and observed abolished energy expenditure difference between HFD- and KD-fed mice (Figures S4D and S4E), corroborating that FGF21 is responsible for the elevated energy expenditure under KD feeding. It is worth noting that the minor unexplained body weight difference between HFD-fed *Gdf15*^{-/-} mice and KD-fed *Gdf15*^{-/-} mice shown in Figure 2C disappeared when the latter were treated with an FGF21 neutralizing antibody (Figure S4F). Collectively, these data suggest that the anti-obesity effects of KD are achieved by orchestration of GDF15-mediated energy intake suppression and FGF21-conferred energy expenditure.

KD-induced GDF15 production originates from the liver

To clarify which organ KD-mediated GDF15 production was mainly derived from, we examined *Gdf15* gene expression in a tissue panel including liver, kidney, heart, skeletal muscle, ileum, and colon, which have been reported as potential sources of circulating GDF15,^{41,59–62} from WT mice treated with either KD or HFD. Compared with HFD controls, markedly increased *Gdf15* mRNA expression was observed in livers of KD-fed mice (Figure 4A). Of note, significantly increased *GDF15* expression was also shown in livers of KD-fed pigs (Figure S5A). Further *in situ* hybridization studies demonstrated strong *Gdf15* expression in mouse hepatocytes (Figures 4B and S5B), suggesting that KD-induced GDF15 elevation was principally from the liver.

To investigate whether KD induces hepatic GDF15 production *in vivo*, we knocked down hepatic *Gdf15* by AAV8 in mice (Figure 4C) and found KD feeding was unable to increase plasma GDF15 in AAV-*Gdf15* mice (Figures 4D and 4E), suggesting that KD induces hepatic GDF15 production. We next investigated the effect of hepatic *Gdf15* on the obesity management effect of KD and observed that upon hepatic *Gdf15* knockdown, the suppression of energy intake and the subsequent body weight loss by KD feeding were markedly reduced (Figures 4F and 4G). The beneficial effects of KD on glucose tolerance and insulin sensitivity disappeared in AAV-*Gdf15* mice, showing comparable levels of glucose-mediated whole-body glucose disposal as well as insulin-stimulated glucose uptake in KD-fed mice and HFD controls (Figures 4H–4K). The fat-reducing effect of KD was markedly diminished in mice receiving AAV-*Gdf15* (Figure 4L). We therefore conclude that the liver is the main site for KD-induced GDF15 production.

Hepatic PPAR γ directly regulates the transcription of *Gdf15*

To investigate the transcriptional regulation of KD-induced hepatic GDF15, we performed RNA sequencing (RNA-seq)

(B) Cumulative energy intake (kcal) in *Gdf15*^{+/+} (left) and *Gdf15*^{-/-} mice (right).

(C) Body weight changes (%).

(D) Weights of iWAT and eWAT.

(E) Liver weight.

(F) Plasma levels of TGs.

(G) Plasma levels of ALT and AST.

(H) Hepatic TG contents.

(I and J) Insulin tolerance test (ITT) and its area under the curve (AUC) (on day 18).

(K and L) Glucose tolerance test (GTT) and its AUC (on day 24).

Data points show individual mice. *Gdf15*^{+/+} (HFD, n = 6; KD, n = 6) and *Gdf15*^{-/-} (HFD, n = 6; KD, n = 5). Data are presented as mean \pm SEM. *p < 0.05, **p < 0.01, ***p < 0.001.

See also Figures S2–S4.

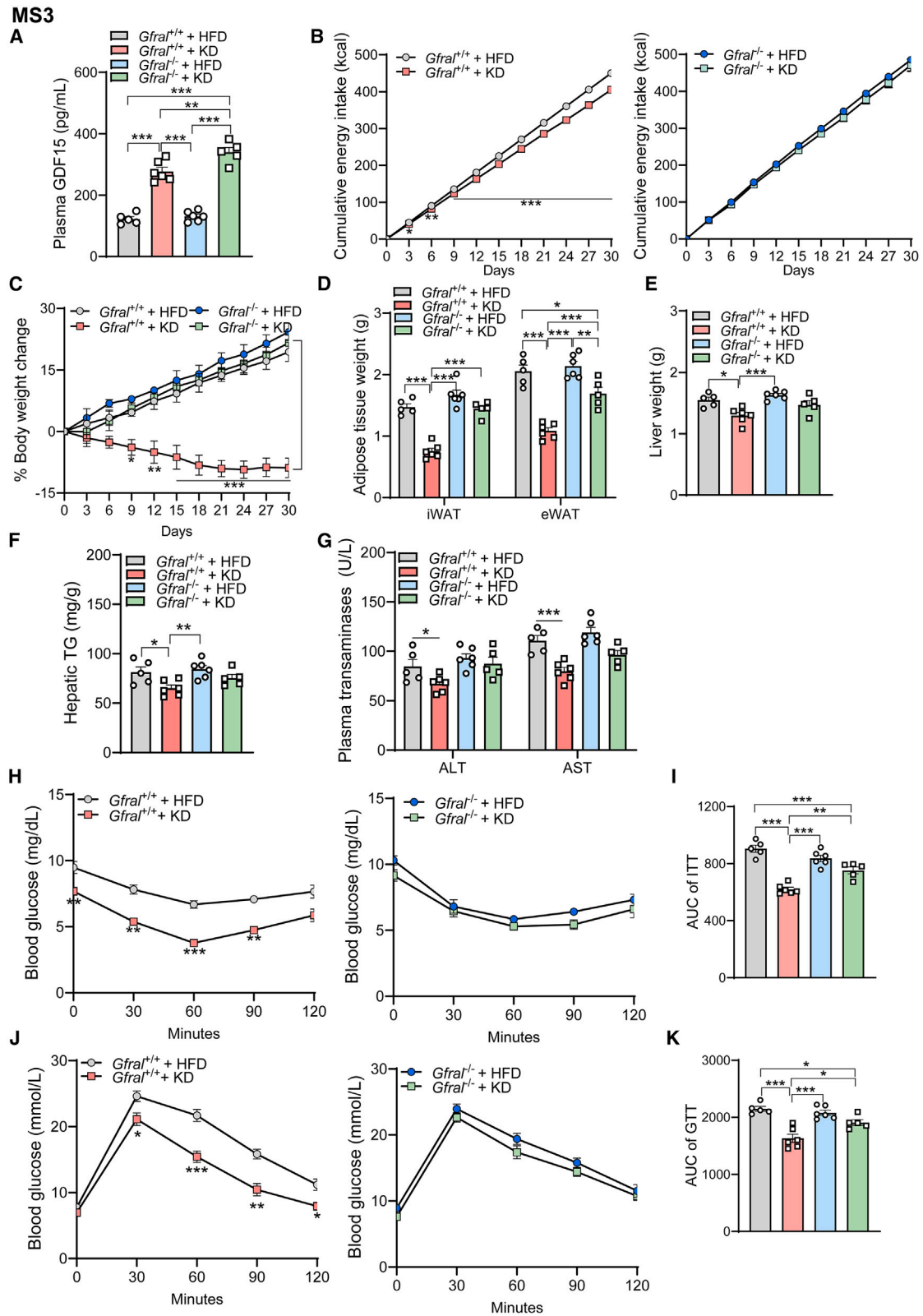


Figure 3. GFRAL is required for the weight-loss effects of KD

Mouse study 3 (MS3): WT and $Gfral^{-/-}$ mice were under HFD or KD feeding for 30 days.

(A) Plasma levels of GDF15 on day 18.

(legend continued on next page)

analysis in livers of HFD- and KD-fed mice (Figure 5A). KEGG pathway analysis revealed enrichment of differentially expressed genes (DEGs) in multiple pathways, especially the PPAR signaling pathway (Figure 5B), of which fifteen genes, including PPAR γ and its targets, were markedly upregulated upon KD feeding (Figure 5C). These results were validated by qPCR analysis (Figure S5C). PPARs constitute a subfamily of nuclear receptors with three members: PPAR α , PPAR γ , and PPAR β/δ .⁶³ Here we noticed a marked increase only for *Ppar γ* mRNA in livers of KD-fed mice (Figure 5D), with no obvious changes for the expression of *Ppar α* and *Ppar β/δ* (Figures S5D and S5E). Also, we found a marked increase for PPAR γ mRNA in livers of KD-fed pig (Figure S5F). Protein levels of PPAR γ were also increased in livers of KD-fed mice (Figure 5E). Together, these results indicate a possible correlation between PPAR γ and GDF15.

To investigate whether the transcription factor PPAR γ directly regulates the transcription of *Gdf15*, we analyzed ~2 kb of the *Gdf15* promoter sequence and identified four putative PPAR-responsive elements (Figure 5F). Luciferase assays showed marked activation of *Gdf15* promoter by PPAR γ expression in hepatocytes (AML12) (Figures 5G and 5H). We also showed that PPAR γ binds to its conserved transcription binding site in the promoter region of *Gdf15* by ChIP-qPCR analysis (Figure 5I). Furthermore, we generated two luciferase reporters driven by WT *Gdf15* promoter and transcription binding site mutant *Gdf15* promoter (Figure 5J). PPAR γ overexpression significantly enhanced WT *Gdf15* promoter-reporter activity but had no effect on that of the mutant form (Figure 5K). Finally, a ChIP assay was carried out to further test the *in vivo* binding of PPAR γ to the *Gdf15* promoter, which was greatly enhanced in livers of KD-fed mice (Figures S6A–S6F). These data imply that PPAR γ functions as a transcription factor to promote *Gdf15* transcription and expression.

To further determine whether hepatocytes are capable of responding to PPAR γ to increase GDF15, we incubated a murine hepatocyte cell line, AML12, with the PPAR γ agonist rosiglitazone and found induction of GDF15 release into the medium and an elevation of *Gdf15* mRNA expression in hepatocytes (Figures 5L and 5M). We then overexpressed *Ppar γ* in AML12 cells and found increased GDF15 release into the medium and *Gdf15* mRNA expression (Figures 5N and 5O). Consistently, in human primary hepatocytes, either rosiglitazone treatment or PPAR γ overexpression significantly increased GDF15 release into the medium and *GDF15* mRNA expression (Figures S7A–S7D). Given that PPAR γ is highly expressed in adipocytes,⁶⁴ we further examined whether adipose PPAR γ functions in a similar way as hepatic PPAR γ . Contrary to the results from hepatocytes, medium

GDF15 was almost undetectable in differentiated 3T3-L1 cells treated with either rosiglitazone or overexpression of *Ppar γ* (Figures S7E and S7F), excluding a similar regulatory mechanism of GDF15 transcription and production in adipocytes. Also, several studies including ours have shown that hepatic integrated stress response (ISR) upregulates GDF15 expression.^{31,41,65} We thus examined whether KD-induced GDF15 expression involves ISR activation by detecting hepatic protein levels of ATF4 and CHOP, key transcriptional regulators of ISR. Their levels were similar between KD-fed mice and their HFD controls (Figures S5G and S5H), excluding a potential involvement of ISR in the production of hepatic GDF15. Together, these results demonstrate that *Ppar γ* upregulates *Gdf15* expression in a hepatocyte-specific manner.

Hepatic Ppar γ -deficient mice show low levels of plasma GDF15 and abolished obesity management of KD

To better understand the relationship between hepatic PPAR γ and GDF15 production *in vivo*, we first generated hepatic *Ppar γ* knockdown mice by AAV8 (Figure 6A). KD-induced hepatic *Gdf15* mRNA expression and secretion were drastically reduced when receiving AAV8-*Ppar γ* shRNA (Figures 6B and 6C) in contrast to scramble shRNA. The weight loss effects of KD were markedly reduced upon hepatic *Ppar γ* knockdown (Figure 6D). We further tested the obesity management effects of KD in liver-specific *Ppar γ* knockout (*Ppar γ ^{Δ Hep}*) mice (Figure 6E) and found KD-induced GDF15 secretion in WT mice, but not in *Ppar γ ^{Δ Hep}* mice (Figure 6F). Contrary to WT mice, which lost weight with KD feeding, *Ppar γ ^{Δ Hep}* mice gained weight (Figure 6G). Accordingly, suppression of energy intake and reduction of fat mass by KD feeding were abolished in *Ppar γ ^{Δ Hep}* mice (Figures 6H and 6I). KD feeding markedly reduced plasma levels of TGs, hepatic lipid content, and liver weight in WT mice, which were largely abrogated in *Ppar γ ^{Δ Hep}* mice (Figures 6J–6L). Moreover, the beneficial effects of KD on glucose tolerance and insulin sensitivity shown in WT mice disappeared with hepatic *Ppar γ* deletion, showing comparable levels of glucose-mediated whole-body glucose disposal as well as insulin-stimulated glucose uptake in KD-treated mice and vehicle controls (Figures 6M and 6N). Together, these results demonstrate that hepatic PPAR γ is required for the obesity management effects of KD.

Hepatic *Gdf15* overexpression or recombinant GDF15 administration rescued the defective metabolic benefits of KD in *Ppar γ ^{Δ Hep}* mice

To establish whether the abolished beneficial effects of KD in *Ppar γ ^{Δ Hep}* mice were due to decreased hepatic *Gdf15*

(B) Cumulative energy intake (kcal) in *Gf15*^{+/+} (left) and *Gf15*^{-/-} mice (right).

(C) Body weight changes (%).

(D) Weights of iWAT and eWAT.

(E) Liver weight.

(F) Hepatic TG contents.

(G) Plasma levels of ALT and AST.

(H and I) ITT and its AUC (on day 18).

(J and K) GTT and its AUC (on day 24).

Gf15^{+/+} (HFD, n = 5; KD, n = 6) and *Gf15*^{-/-} (HFD, n = 6; KD, n = 5). Data points show individual mice. Data are presented as mean \pm SEM. *p < 0.05, **p < 0.01, ***p < 0.001.

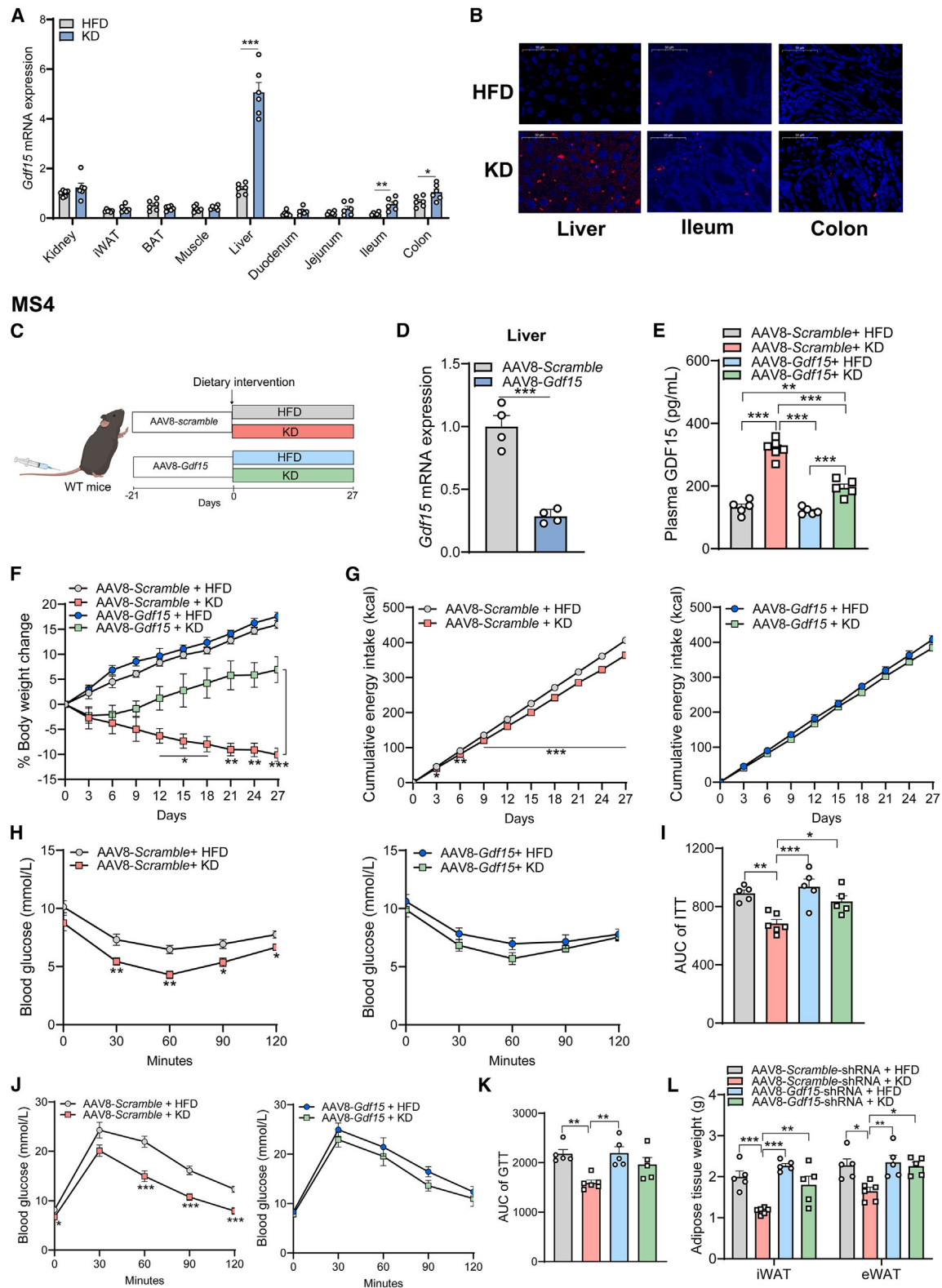


Figure 4. Circulating GDF15 during KD dietary intervention mainly originates from liver

(A) *Gdf15* mRNA expression in different tissues of mice with 15 days of dietary intervention was analyzed by RT-qPCR and normalized to that in kidney. (B) *In situ* hybridization for *Gdf15* mRNA (red spots). Representative images from the mice treated with HFD or KD. Mice were from groups described in (A) (n = 6). (C–L) Mouse study 4 (MS4).

(legend continued on next page)

expression and low circulating GDF15, we performed *in vivo* rescue experiments to restore *Gdf15* expression in the liver (Figure 7A). Compared with *Ppar γ ^{ΔHep}* mice receiving AAV-vector, hepatic overexpression of *Gdf15* caused a significant induction of GDF15 secretion in mice (Figure 7B), restoring the defective suppression of energy intake, weight loss, and fat reduction by KD feeding (Figures 7C–7E). Similarly, gain of GDF15 function in the liver restored the impaired glucose tolerance and reduced hepatic TG content in KD-fed *Ppar γ ^{ΔHep}* mice (Figures 7F and 7G).

We further used recombinant GDF15 to test whether systemic elevation of circulating GDF15 is able to restore the impaired beneficial effects of KD in *Ppar γ ^{ΔHep}* mice (Figures 7H and 7I). We found that recombinant GDF15 administration effectively restored the blunted suppression of energy intake (Figure 7J); the defective reduction in body weight, fat mass, and hepatic TG content (Figures 7K–7M); and the impaired glucose tolerance (Figure 7N) in KD-fed *Ppar γ ^{ΔHep}* mice. Collectively, these results demonstrate that hepatic PPAR γ governs KD-mediated metabolic benefits through upregulation of GDF15 production.

DISCUSSION

Recent clinical trials support that KD could be efficient for the management of body weight and body composition.^{7,66} The principal aim of our work was to understand if and how GDF15 might be involved in KD-mediated body weight control. Herein, we present a body of data from cells to mice, pigs, and humans that establish a major role for GDF15 in the mediation of the beneficial effects of KD on weight loss. We found that KD feeding reduces body weight in obese mice, preclinical model pigs, and obese individuals accompanied by elevated circulating GDF15. Deficiency of GDF15 or GFRAL in mice abolishes the metabolic benefits of KD, corroborating that the GDF15-GFRAL axis is an essential signaling node for KD. We further demonstrate that hepatic PPAR γ governs the transcription and production of GDF15 in KD-fed mice and human primary hepatocytes. These findings provide a previously unexplored molecular basis for KD-mediated obesity management.

Among the multiple nutritional stimuli, KD is relatively specific for the induction of GDF15. GDF15 is not a “sensitive/quick-response” hormone compared to its appetite suppressor peers such as leptin and enteroendocrine hormones such as GLP-1, which fluctuate with short-term fasting or HFD feeding.^{67,68} Here, we showed that among the four widely tested obesity man-

agement diets, Mediterranean diet, low-fat diet, high-protein diet, and low-glycemic-index diet, as well as two fasting regimes (every-other-day fasting and time-restricted feeding),^{3,69,70} KD is the only diet capable of inducing GDF15 expression and production within a short-term feeding regime, revealing a distinct mechanism underlying KD-mediated obesity management from those of other types of diets or dietary regimes.^{53,71–73}

Of note, unelevated circulating GDF15 levels were shown in a previous KD intervention study during the investigation of the effect of KD on liver metabolism in participants with obesity.⁷⁴ This is in contrast to our results, and several factors may contribute to this discrepancy:

- (1) Different dietary intervention duration. In Luukkonen’s study, participants with obesity consumed 6 days of KD,⁷⁴ while in this study the intervention trial lasted for 2 weeks.
- (2) Number of participants. In Luukkonen’s study, data from 10 valid participants with obesity were analyzed, whereas 19 out of 30 participants were included for data analysis after accounting for withdrawals in this study.
- (3) Race/ethnicity. It is well accepted that genetic background influences an individual’s susceptibility to dietary intervention and the subsequent plasma parameters.^{75,76} In this study, all participants are Chinese Han ethnicity. Although Luukkonen et al. did not provide information on race/ethnicity of the participants, given the fact that the study was conducted in a multicultural environment,⁷⁴ the race/ethnicity of the population from the two cohorts is likely distinct. Thus, further investigation is needed to determine whether these factors affect the effect of KD on circulating levels of GDF15.

We also noticed the discrepancy in the effect of fasting on circulating levels of GDF15. Two independent studies showed that a 24-h fast had no effects on circulating levels of GDF15 in mice.^{65,77} Our result that every-other-day fasting is unable to elevate circulating levels of GDF15 in mice is consistent with these conclusions. Nonetheless, Zhang et al. reported augmented circulating GDF15 levels in 24-h-fasting mice.⁷⁸ These seemingly contradictory results may be attributable to factors including but not limited to age, gender, and/or diet of mice and thus merit further investigation.

What are the general consequences of GDF15 elevation in KD feeding? In this study, we found that KD as a nutritional stimulus elevated circulating GDF15 in obese mice, miniature pigs, and people with obesity, suggesting it is universal across species. Another application of KD in humans is for the treatment of

(C) Schematic diagram of mouse treatment. Mice were intravenously injected once with adenovirus (AAV8-*Scramble* or AAV8-*Gdf15*). After 21 days, mice were given either an HFD or KD for 27 days. Thus, four groups of mice (HFD + AAV8-*Scramble*, KD + AAV8-*Scramble*, HFD + AAV8-*Gdf15*, and KD + AAV8-*Gdf15*) were studied here.

(D) Hepatic *Gdf15* mRNA expression (n = 4 per group).

(E) Plasma levels of GDF15 on day 9.

(F) Body weight changes of mice (%).

(G) Cumulative energy intake (kcal).

(H and I) ITT and its AUC (performed on day 8).

(J and K) GTT and its AUC (on day 14).

(L) Weight of iWAT and eWAT.

AAV8-*Scramble* (HFD, n = 5; KD, n = 6) and AAV8-*Gdf15* (HFD, n = 5; KD, n = 5). Data points show individual mice. Data are presented as mean \pm SEM. *p < 0.05, **p < 0.01, ***p < 0.001.

See also Figure S5.

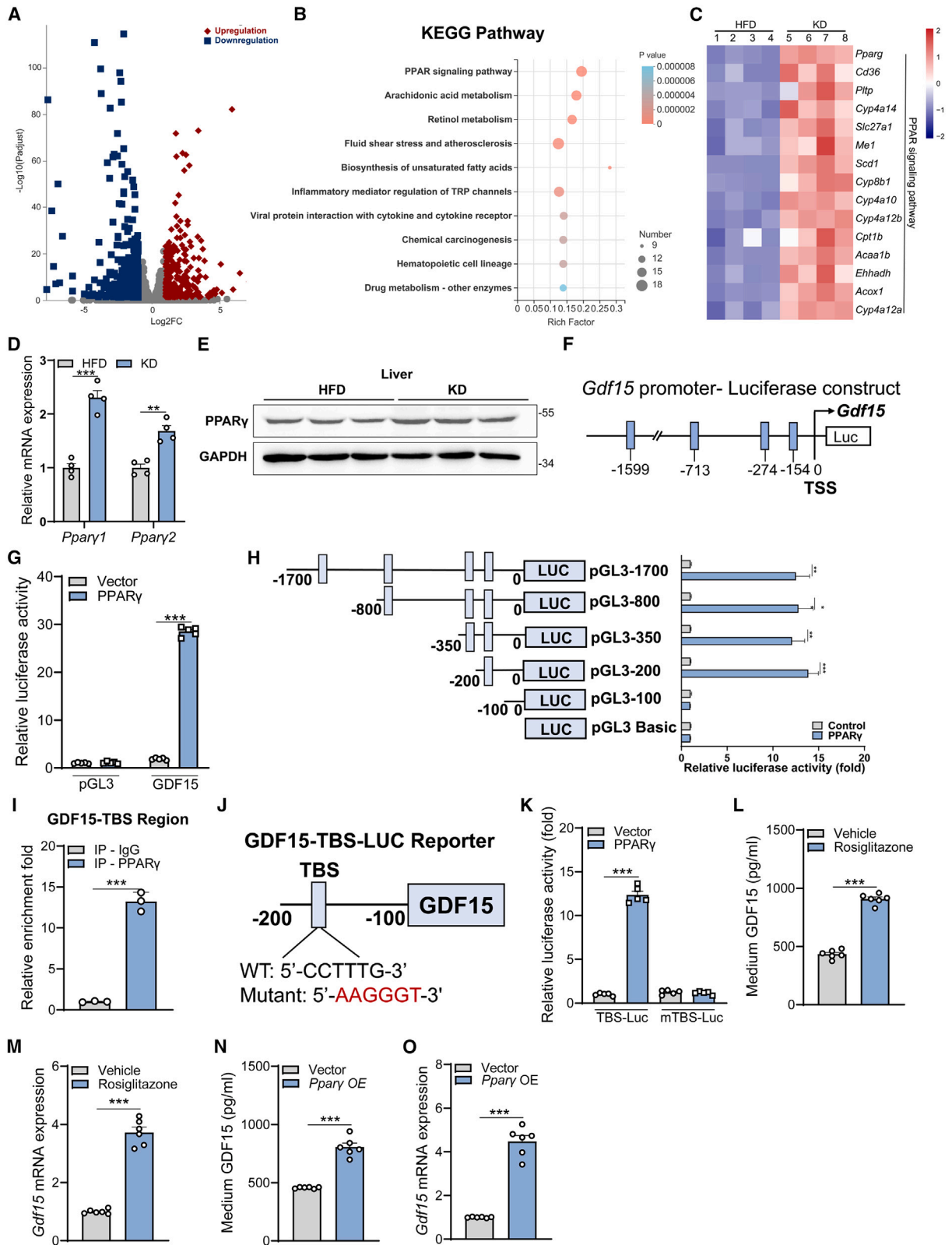


Figure 5. Liver but not adipose tissue *Ppar* γ upregulates *Gdf15* expression
 (A) Volcano plots: differentially expressed genes (DEGs) in livers of mice fed KD versus HFD.
 (B) KEGG pathway analysis. PPAR signaling pathway was enriched on the top.

(legend continued on next page)

epilepsy^{8,12}: does elevation of GDF15 also occur in these patients, and if so, does this contribute to the reported weight loss in some cases? Moreover, there are over 400 registered clinical trials to test the effects of KD in different conditions, including cancers, viral infection, and aging ([ClinicalTrials.gov](https://www.clinicaltrials.gov) database). It is highly recommended to monitor circulating GDF15 levels under these trials based on at least one piece of convincing evidence that detrimental levels of GDF15 were shown in cancer patients, which correlates with cachexia and reduced survival.^{79,80} Clinical trials of KD in these patients may worsen their pathologies. Therefore, if KD consumption generally elevates circulating GDF15, in some settings this is likely to be advantageous while there are clearly exceptions where it is not.

Management of obesity and its associated metabolic disorders could be achieved by reduced energy intake and/or increased energy expenditure. Previous studies showed increased energy expenditure in KD-mediated obesity management in mice.^{46,81} Nonetheless, in this study, we provide evidence that increased energy expenditure, mediated by FGF21, accounts for a relatively small contribution to this process. We corroborated that GDF15-conferred reduced energy intake is a major contributor for obesity management effects of KD, by using GDF15- and its receptor GFRAL-deficient mice, as well as a GDF15 neutralizing antibody. We discovered a synergic action between GDF15 and FGF21 in the obesity management of KD by giving *Gdf15*^{-/-} mice an FGF21 neutralizing antibody and observed completely abolished effects of KD on weight loss. In line with this, the orchestration of GDF15 and FGF21 was also shown in the amelioration of diet-induced obesity and metabolic disorders by the deadenylase CNOT6L.⁸² Whether this synergic action is also implicated in other types of diet or gene-regulated obesity merits further investigation.

What is the upstream regulator of the elevated levels of GDF15 in KD feeding conditions? To answer this question, we investigated the transcriptional regulation of GDF15 and provided evidence that hepatic PPAR γ governs KD-induced GDF15 transcription and production. Intriguingly, PPAR γ , a highly expressed transcription factor in adipocytes, is unable to upregulate GDF15 expression in adipocytes. Consistent with this, recent studies from Savage's lab revealed that adipocytes are

not the cellular source of GDF15.⁸³ Furthermore, PPAR γ is also expressed in the intestine,⁸⁴ where metformin-induced GDF15 was reportedly derived from⁵⁹; whether intestinal PPAR γ also controls GDF15 transcription and production warrants further investigation. Besides PPAR γ , other transcription factors such as ATF3, NRF2, and p53 were shown to regulate GDF15 expression in myotubes,⁸⁵ hepatocytes,⁸⁶ and prostate cancer cells,⁸⁷ respectively. These findings suggest a cell-type-specific regulatory mechanism of GDF15, which opens a new area of research in future studies.

Limitations of the study

This study identified that GDF15 is crucial for KD-mediated obesity management, whose contribution was explored by employing GDF15-deficient mice and a GDF15 neutralizing antibody. Our data support that KD increases GDF15 levels, which originate from activation of hepatic PPAR γ -governed GDF15 transcription and production, thereby regulating energy intake and body weight. Nonetheless, our work has several limitations. First, we only addressed the role of GDF15 in KD-mediated weight loss in male animals for a relatively short period of time (2 weeks to 1 month). Studies with female animals are needed to gain a more comprehensive understanding of this regulatory mechanism. Second, binding of other PPAR isoforms such as PPAR α and/or PPAR β/δ to *Gdf15* in mouse liver under KD feeding condition is not totally excluded and needs further investigation. Third, although we demonstrated elevated circulating GDF15 and reduced body weight in individuals with obesity under KD intervention, the translational relevance of the work would be improved if tested in a large cohort of participants with obesity.

STAR★METHODS

Detailed methods are provided in the online version of this paper and include the following:

- KEY RESOURCES TABLE
- RESOURCE AVAILABILITY
 - Lead contact
 - Materials availability
 - Data and code availability

(C) Heatmap showing the individual DEG that was enriched in PPAR signaling pathway (n = 4).

(D) mRNA expression of *Ppar γ 1* and *Ppar γ 2* in livers from HFD- or KD-fed mice (n = 4).

(E) Protein levels of PPAR γ in livers of mice, representative of three independent experiments.

(F) The luciferase construct of the 5'-flanking region of mouse *Gdf15*, containing putative PPAR γ -responsive elements (PPRE, blue squares). TSS, transcription start site.

(G) Luciferase assay using mouse *Gdf15* promoter. The promoter activity was shown by relative luciferase activity with overexpression of *Ppar γ* in AML12 cells (n = 5).

(H) Cell-based reporter assays were performed in AML12 cells transfected with the indicated *Gdf15*-luciferase reporter plasmids in the presence of control plasmid or *Ppar γ* expression plasmid.

(I) ChIP-qPCR analysis of PPAR γ transcription binding site on *Gdf15* promoter region was performed with overexpression of *Ppar γ* in AML12 cells (n = 3).

(J) Schematic illustration of the promoter structure of *Gdf15* with potential PPAR γ binding site. The WT and PPAR γ binding site mutant sequences are indicated. TBS, transcription binding site.

(K) Luciferase analysis showing the effects of PPAR γ on WT or mutant GDF15-PPAR γ binding site (n = 5). The proximal promoter region of *Gdf15* was amplified by qPCR in liver.

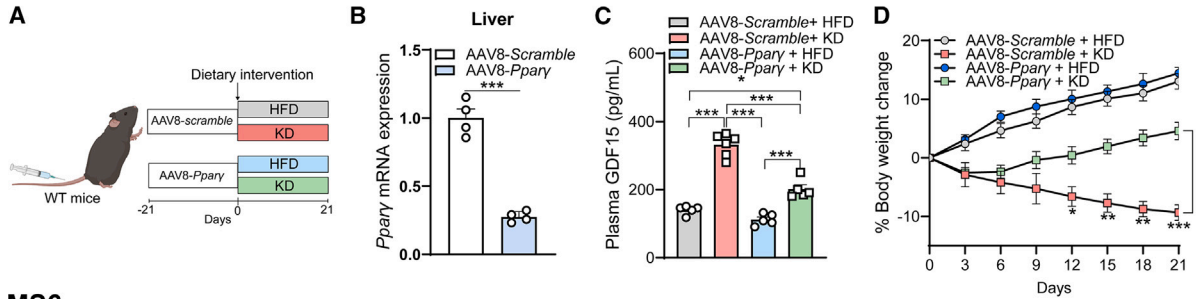
(L and M) Relative *Gdf15* expression and GDF15 release in AML12 cells treated with 10 μ M rosiglitazone for 48 h (n = 6).

(N and O) Relative *Gdf15* expression and GDF15 release in *Ppar γ* -overexpressing AML12 cells (n = 6).

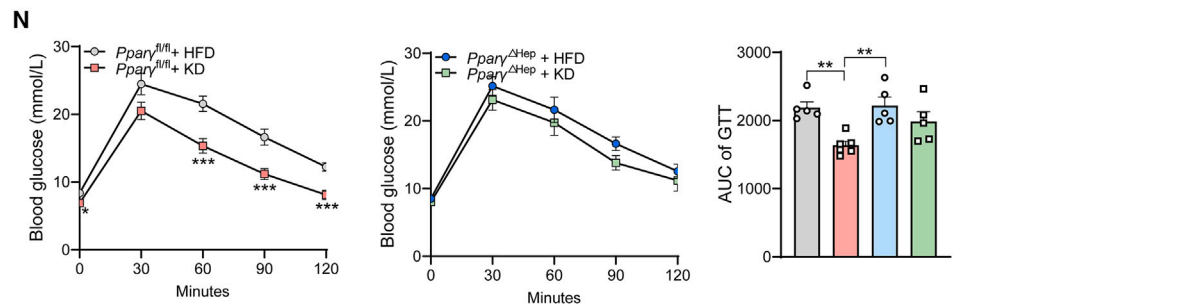
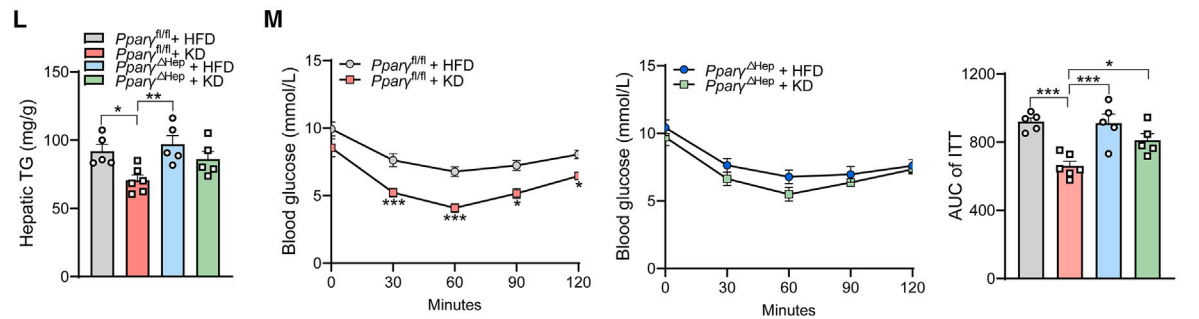
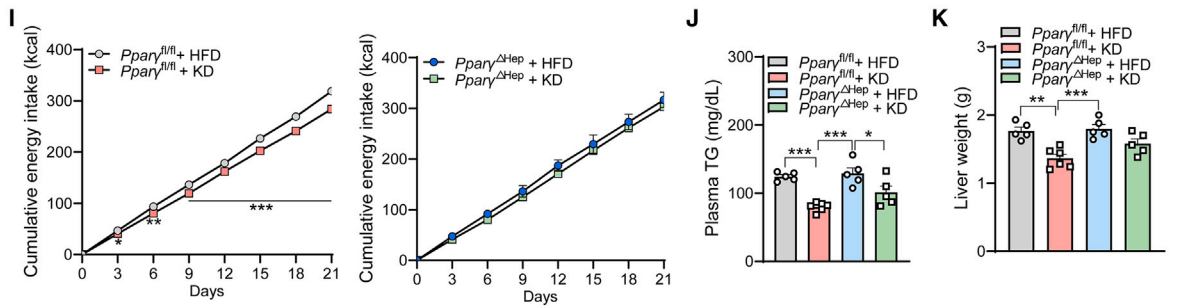
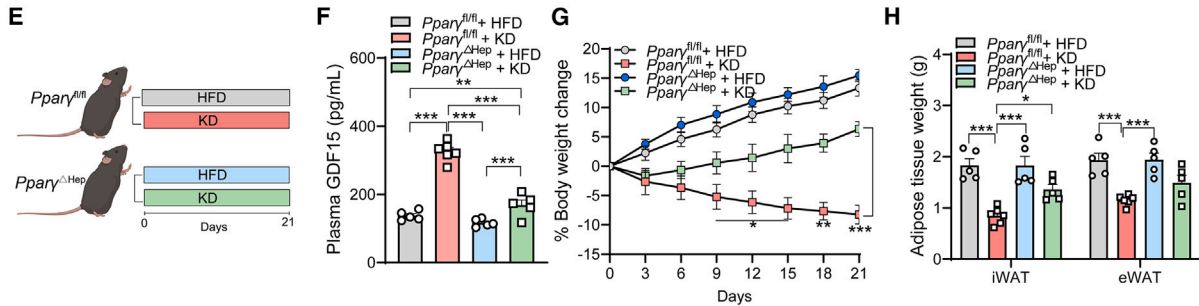
Data are presented as mean \pm SEM.

See also [Figures S5–S7](#).

MS5



MS6



(legend on next page)

● EXPERIMENTAL MODEL AND STUDY PARTICIPANT DETAILS

- Human study: Effect of KD on humans
- Animal studies

● METHOD DETAILS

- Pig study: Effect of KD on pigs
- Mouse study 1 (MS1): Effect of KD on mice
- Mouse study 2 (MS2): HFD and KD, *Gdf15*^{-/-} mice
- Mouse study 3 (MS3): HFD and KD, *Gfral*^{-/-} mice
- Mouse study 4 (MS4): AAV8-mediated *Gdf15* knockdown
- Mouse study 5 (MS5): AAV8-mediated *Pparγ* knockdown
- Mouse study 6 (MS6): *Pparγ*^{ΔHep} mice
- Mouse study 7 (MS7): *Pparγ*^{ΔHep} mice with GDF15 overexpression
- Mouse study 8 (MS8): *Pparγ*^{ΔHep} mice with recombinant GDF15 administration
- Mouse study 9 (MS9): Effects of different diets on plasma levels of GDF15
- Mouse study 10 (MS10): Effects of different fasting regimes on plasma levels of GDF15
- Mouse study 11 (MS11): GDF15 antibody validation
- Mouse study 12 (MS12): GDF15 antibody neutralization in mice
- Mouse study 13 (MS13): Pair feeding experiment
- Mouse study 14 (MS14): *Gdf15*^{-/-} mice with FGF21 antibody neutralization
- Plasma analysis
- Liver TG analysis
- Calorimetry
- Real-time qPCR and Western blots
- *In situ* hybridization
- GTT and ITT
- RNA-sequencing and bioinformatic analyses
- Cell culture
- Plasmids
- Plasmid transfection and luciferase reporter assay

- Chromatin immunoprecipitation (ChIP) qPCR
- QUANTIFICATION AND STATISTICAL ANALYSIS

SUPPLEMENTAL INFORMATION

Supplemental information can be found online at <https://doi.org/10.1016/j.cmet.2023.11.003>.

ACKNOWLEDGMENTS

We thank Dr. Sir Stephen O’Rahilly (University of Cambridge, UK), Dr. David B. Savage (University of Cambridge, UK), and Dr. Gregory R. Steinberg (McMaster University, Canada) for critical reading and helpful discussions of the manuscript. This work was supported by the National Key Research and Development Program of China (2021YFF1000602 to J.W.W.), National Natural Science Foundation of China (32370569 and 32070602 to J.W.W.), and Shaanxi Science & Technology Program (2023-CX-TD-57 to J.W.W.). Graphical abstract created with biorender.com.

AUTHOR CONTRIBUTIONS

J.F.L. and J.W.W. conceived the study. J.F.L., M.Q.Z., B.X., N.N.Z., and X.M.L. designed and performed the majority of the experiments. J.F.L., M.Q.Z., N.N.Z., X.P.L., H.L., R.X.Z., and J.Y.X. analyzed the data. J.F.L., M.Q.Z., and J.W.W. wrote and revised the manuscript. B.X., X.M.L., and J.W.W. contributed to the discussion and critical review of the manuscript. H.Y., Y.Q.Z., X.M.L., and J.W.W. provided crucial insight into the study. X.M.L. and J.W.W. supervised the project. All authors reviewed the final manuscript.

DECLARATION OF INTERESTS

The authors declare no competing interests.

INCLUSION AND DIVERSITY

We support inclusive, diverse, and equitable conduct of research.

Received: January 31, 2023

Revised: July 27, 2023

Accepted: November 10, 2023

Published: December 5, 2023

Figure 6. Hepatic *Pparγ*-deficient mice show low levels of plasma GDF15 and largely abolished obesity management of KD

(A–D) Mouse study 5 (MS5).

(A) Schematic diagram of mouse treatment. Mice were intravenously injected once with adenovirus (AAV8-*Scramble* or AAV8-*Pparγ*). After 21 days, mice were given either an HFD or KD for 21 days. Thus, four groups of mice (HFD + AAV8-*Scramble*, HFD + AAV8-*Pparγ*, KD + AAV8-*Scramble*, and KD + AAV8-*Pparγ*) were studied here.

(B) Hepatic *Pparγ* mRNA expression (n = 4).

(C) Plasma levels of GDF15 on day 9.

(D) Body weight changes in mice (%).

AAV8-*Scramble* (HFD, n = 5; KD, n = 6) and AAV8-*Pparγ* (HFD, n = 5; KD, n = 5).

(E–N) Mouse study 6 (MS6).

(E) Schematic diagram of mouse feeding. *Pparγ*^{ΔHep} and *Pparγ*^{fl/fl} mice were under HFD or KD feeding for 21 days.

(F) Plasma levels of GDF15 on day 9.

(G) Body weight changes (%).

(H) Weight of iWAT and eWAT.

(I) Cumulative energy intake (kcal) in *Pparγ*^{fl/fl} (left) and *Pparγ*^{ΔHep} mice (right).

(J) Plasma levels of TGs.

(K) Liver weight.

(L) Hepatic TG content.

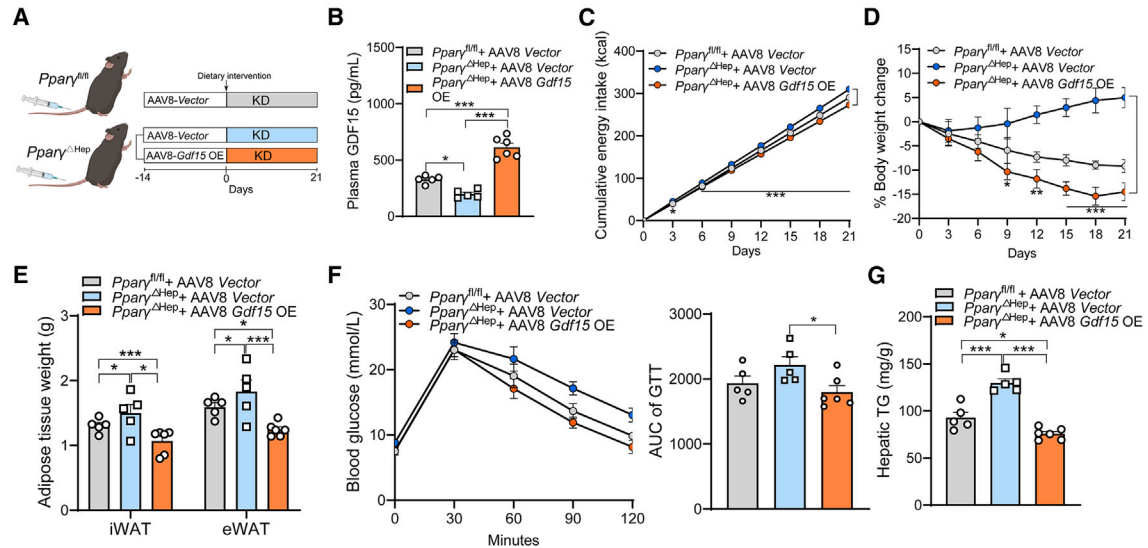
(M) ITT performed after 9 days of feeding and its AUC.

(N) GTT performed after 15 days of feeding and its AUC.

Pparγ^{fl/fl} (HFD, n = 5; KD, n = 6) and *Pparγ*^{ΔHep} (HFD, n = 5; KD = 5).

Data are presented as mean ± SEM. *p < 0.05, **p < 0.01, ***p < 0.001. TG, triglyceride.

MS7



MS8

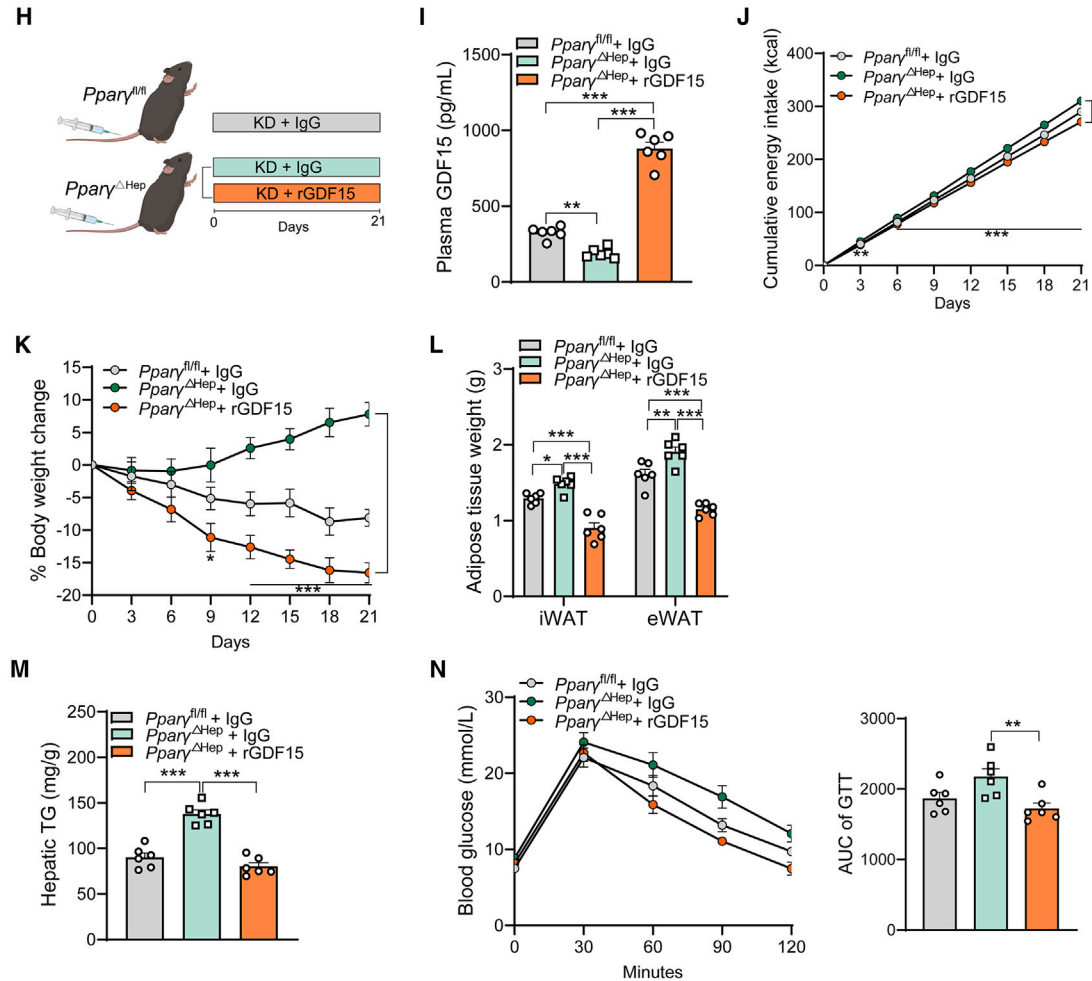


Figure 7. Defective body weight-lowering effects of KD in *Ppar γ ^{Δ Hep}* mice could be restored by hepatic *Gdf15* overexpression or rGDF15 (A–G) Mouse study 7 (MS7).

(A) Schematic diagram of mouse treatment. *Ppar γ ^{Δ Hep}* and *Ppar γ ^{fl/fl}* mice were treated with AAV8-encoding GDF15 or vector, followed by KD feeding for 21 days.

(legend continued on next page)

REFERENCES

- Blüher, M. (2019). Obesity: global epidemiology and pathogenesis. *Nat. Rev. Endocrinol.* *15*, 288–298.
- Mozaffarian, D. (2020). Dietary and policy priorities to reduce the global crises of obesity and diabetes. *Nat. Food* *1*, 38–50.
- Chao, A.M., Quigley, K.M., and Wadden, T.A. (2021). Dietary interventions for obesity: clinical and mechanistic findings. *J. Clin. Invest.* *131*, e140065.
- Clifton, P.M. (2008). Dietary treatment for obesity. *Nat. Clin. Pract. Gastroenterol. Hepatol.* *5*, 672–681.
- Zhu, H., Bi, D., Zhang, Y., Kong, C., Du, J., Wu, X., Wei, Q., and Qin, H. (2022). Ketogenic diet for human diseases: the underlying mechanisms and potential for clinical implementations. *Signal Transduct. Target. Ther.* *7*, 11.
- Abbasi, J. (2018). Interest in the ketogenic diet grows for weight loss and type 2 diabetes. *JAMA* *319*, 215–217.
- Drabińska, N., Wiczkowski, W., and Piskula, M.K. (2021). Recent advances in the application of a ketogenic diet for obesity management. *Trends Food Sci. Technol.* *110*, 28–38.
- Neal, E.G., Chaffe, H., Schwartz, R.H., Lawson, M.S., Edwards, N., Fitzsimmons, G., Whitney, A., and Cross, J.H. (2008). The ketogenic diet for the treatment of childhood epilepsy: a randomised controlled trial. *Lancet Neurol.* *7*, 500–506.
- Wiers, C.E., Vendruscolo, L.F., van der Veen, J.W., Manza, P., Shokri-Kojori, E., Kroll, D.S., Feldman, D.E., McPherson, K.L., Biesecker, C.L., Zhang, R., et al. (2021). Ketogenic diet reduces alcohol withdrawal symptoms in humans and alcohol intake in rodents. *Sci. Adv.* *7*, eabf6780.
- Hopkins, B.D., Goncalves, M.D., and Cantley, L.C. (2016). Obesity and cancer mechanisms: cancer metabolism. *J. Clin. Oncol.* *34*, 4277–4283.
- Newman, J.C., Covarrubias, A.J., Zhao, M., Yu, X., Gut, P., Ng, C.P., Huang, Y., Haldar, S., and Verdin, E. (2017). Ketogenic diet reduces midlife mortality and improves memory in aging mice. *Cell Metab.* *26*, 547–557.e8.
- Cervenka, M.C., Hocker, S., Koenig, M., Bar, B., Henry-Barron, B., Kossoff, E.H., Hartman, A.L., Probasco, J.C., Benavides, D.R., Venkatesan, A., et al. (2017). Phase I/II multicenter ketogenic diet study for adult superrefractory status epilepticus. *Neurology* *88*, 938–943.
- Barrea, L., Caprio, M., Tuccinardi, D., Moriconi, E., Di Renzo, L., Muscogiuri, G., Colao, A., and Savastano, S.; Obesity Programs of Nutrition, Education, Research and Assessment (OPERA) group (2022). Could ketogenic diet "starve" cancer? Emerging evidence. *Crit. Rev. Food Sci. Nutr.* *62*, 1800–1821.
- Casanueva, F.F., Castellana, M., Bellido, D., Trimboli, P., Castro, A.I., Sajoux, I., Rodríguez-Carnero, G., Gomez-Arbelaiz, D., Crujeiras, A.B., and Martínez-Olmos, M.A. (2020). Ketogenic diets as treatment of obesity and type 2 diabetes mellitus. *Rev. Endocr. Metab. Disord.* *21*, 381–397.
- Goldberg, E.L., Molony, R.D., Kudo, E., Sidorov, S., Kong, Y., Dixit, V.D., and Iwasaki, A. (2019). Ketogenic diet activates protective gammadelta T cell responses against influenza virus infection. *Sci. Immunol.* *4*, eaav2026.
- Torres, J.A., Kruger, S.L., Broderick, C., Amarikhagva, T., Agrawal, S., Dodam, J.R., Mrug, M., Lyons, L.A., and Weimbs, T. (2019). Ketosis ameliorates renal cyst growth in polycystic kidney disease. *Cell Metab.* *30*, 1007–1023.e5.
- Weber, D.D., Aminzadeh-Gohari, S., Tulipan, J., Catalano, L., Feichtinger, R.G., and Kofler, B. (2020). Ketogenic diet in the treatment of cancer - where do we stand? *Mol. Metab.* *33*, 102–121.
- Ferrer, M., Mourikis, N., Davidson, E.E., Kleeman, S.O., Zaccaria, M., Habel, J., Rubino, R., Gao, Q., Flint, T.R., Young, L., et al. (2023). Ketogenic diet promotes tumor ferroptosis but induces relative corticosterone deficiency that accelerates cachexia. *Cell Metab.* *35*, 1147–1162.e7.
- McSwiney, F.T., Wardrop, B., Hyde, P.N., Lafountain, R.A., Volek, J.S., and Doyle, L. (2018). Keto-adaptation enhances exercise performance and body composition responses to training in endurance athletes. *Metabolism* *81*, 25–34.
- Ludwig, D.S. (2020). The ketogenic diet: evidence for optimism but high-quality research needed. *J. Nutr.* *150*, 1354–1359. <https://doi.org/10.1093/jn/nxz308>.
- Joshi, S., Ostfeld, R.J., and McMacken, M. (2019). The ketogenic diet for obesity and diabetes-enthusiasm outpaces evidence. *JAMA Intern. Med.* *179*, 1163–1164.
- Bootcov, M.R., Bauskin, A.R., Valenzuela, S.M., Moore, A.G., Bansal, M., He, X.Y., Zhang, H.P., Donnellan, M., Mahler, S., Pryor, K., et al. (1997). MIC-1, a novel macrophage inhibitory cytokine, is a divergent member of the TGF-beta superfamily. *Proc. Natl. Acad. Sci. USA* *94*, 11514–11519.
- Lawton, L.N., Bonaldo, M.F., Jelenc, P.C., Qiu, L., Baumes, S.A., Marcelino, R.A., de Jesus, G.M., Wellington, S., Knowles, J.A., Warburton, D., et al. (1997). Identification of a novel member of the TGF-beta superfamily highly expressed in human placenta. *Gene* *203*, 17–26.
- Paralkar, V.M., Vail, A.L., Grasser, W.A., Brown, T.A., Xu, H., Vukicevic, S., Ke, H.Z., Qi, H., Owen, T.A., and Thompson, D.D. (1998). Cloning and characterization of a novel member of the transforming growth factor-beta/bone morphogenetic protein family. *J. Biol. Chem.* *273*, 13760–13767.
- Keipert, S., and Ost, M. (2021). Stress-induced FGF21 and GDF15 in obesity and obesity resistance. *Trends Endocrinol. Metab.* *32*, 904–915.
- Wang, D., Day, E.A., Townsend, L.K., Djordjevic, D., Jørgensen, S.B., and Steinberg, G.R. (2021). GDF15: emerging biology and therapeutic

(B) Plasma levels of GDF15 on day 9.

(C) Cumulative energy intake (kcal).

(D) Body weight changes (%).

(E) Weight of iWAT and eWAT.

(F) GTT performed after 9 days of KD feeding and its AUC.

(G) Hepatic TG contents.

Ppar γ ^{fl/fl} (AAV8 Scramble, n = 5), *Ppar γ ^{Δ Hep}* (AAV8 Scramble, n = 5), and *Ppar γ ^{Δ Hep}* (AAV8 *Gdf15* OE, n = 6).

(H–N) Mouse study 8 (MS8).

(H) Schematic diagram of mouse treatment. *Ppar γ ^{Δ Hep}* and *Ppar γ ^{fl/fl}* mice fed KD were treated with recombinant GDF15 or control IgG every other day for 21 days.

(I) Plasma levels of GDF15 on day 9.

(J) Cumulative energy intake (kcal).

(K) Body weight changes (%).

(L) Weight of iWAT and eWAT.

(M) Hepatic TG content.

(N) GTT performed after 9 days of KD feeding and its AUC. n = 6 for each group.

Data points show individual mouse. Data are presented as mean \pm SEM. *p < 0.05, **p < 0.01, ***p < 0.001.

- applications for obesity and cardiometabolic disease. *Nat. Rev. Endocrinol.* **17**, 592–607.
27. Lockhart, S.M., Saudek, V., and O'Rahilly, S. (2020). GDF15: a hormone conveying somatic distress to the brain. *Endocr. Rev.* **41**, bnaa007.
 28. Tsai, V.W.W., Husaini, Y., Sainsbury, A., Brown, D.A., and Breit, S.N. (2018). The MIC-1/GDF15-GFRAL pathway in energy homeostasis: implications for obesity, cachexia, and other associated diseases. *Cell Metab.* **28**, 353–368.
 29. Alcazar, J., Frandsen, U., Prokhorova, T., Kamper, R.S., Haddock, B., Aagaard, P., and Suetta, C. (2021). Changes in systemic GDF15 across the adult lifespan and their impact on maximal muscle power: the Copenhagen Sarcopenia Study. *J. Cachexia Sarcopenia Muscle* **12**, 1418–1427.
 30. Eggers, K.M., Kempf, T., Wallentin, L., Wollert, K.C., and Lind, L. (2013). Change in growth differentiation factor 15 concentrations over time independently predicts mortality in community-dwelling elderly individuals. *Clin. Chem.* **59**, 1091–1098.
 31. Aguilar-Recarte, D., Barroso, E., Palomer, X., Wahli, W., and Vázquez-Carrera, M. (2022). Knocking on GDF15's door for the treatment of type 2 diabetes mellitus. *Trends Endocrinol. Metab.* **33**, 741–754.
 32. Wang, D., Jabile, M.J.T., Lu, J., Townsend, L.K., Valvano, C.M., Gautam, J., Batchuluun, B., Tsakiridis, E.E., Lally, J.S., and Steinberg, G.R. (2023). Fatty acids increase GDF15 and reduce food intake through a GFRAL signaling axis. *Diabetes*. <https://doi.org/10.2337/db23-0495>.
 33. Chrysovergis, K., Wang, X., Kosak, J., Lee, S.H., Kim, J.S., Foley, J.F., Travlos, G., Singh, S., Baek, S.J., and Eling, T.E. (2014). NAG-1/GDF-15 prevents obesity by increasing thermogenesis, lipolysis and oxidative metabolism. *Int. J. Obes.* **38**, 1555–1564.
 34. Macia, L., Tsai, V.W.W., Nguyen, A.D., Johnen, H., Kuffner, T., Shi, Y.C., Lin, S., Herzog, H., Brown, D.A., Breit, S.N., and Sainsbury, A. (2012). Macrophage inhibitory cytokine 1 (MIC-1/GDF15) decreases food intake, body weight and improves glucose tolerance in mice on normal & obesogenic diets. *PLoS One* **7**, e34868.
 35. Mullican, S.E., Lin-Schmidt, X., Chin, C.N., Chavez, J.A., Furman, J.L., Armstrong, A.A., Beck, S.C., South, V.J., Dinh, T.Q., Cash-Mason, T.D., et al. (2017). GFRAL is the receptor for GDF15 and the ligand promotes weight loss in mice and nonhuman primates. *Nat. Med.* **23**, 1150–1157.
 36. Mullican, S.E., and Rangwala, S.M. (2018). Uniting GDF15 and GFRAL: therapeutic opportunities in obesity and beyond. *Trends Endocrinol. Metab.* **29**, 560–570.
 37. Breit, S.N., Tsai, V.W.W., and Brown, D.A. (2017). Targeting obesity and cachexia: identification of the GFRAL receptor-MIC-1/GDF15 pathway. *Trends Mol. Med.* **23**, 1065–1067.
 38. Zhang, Y., Zhao, X., Dong, X., Zhang, Y., Zou, H., Jin, Y., Guo, W., Zhai, P., Chen, X., and Kharitonov, A. (2023). Activity-balanced GLP-1/GDF15 dual agonist reduces body weight and metabolic disorder in mice and non-human primates. *Cell Metab.* **35**, 287–298.e4.
 39. Emmerson, P.J., Wang, F., Du, Y., Liu, Q., Pickard, R.T., Gonciarz, M.D., Coskun, T., Hamang, M.J., Sindelar, D.K., Ballman, K.K., et al. (2017). The metabolic effects of GDF15 are mediated by the orphan receptor GFRAL. *Nat. Med.* **23**, 1215–1219.
 40. Yang, L., Chang, C.C., Sun, Z., Madsen, D., Zhu, H., Padkjær, S.B., Wu, X., Huang, T., Hultman, K., Paulsen, S.J., et al. (2017). GFRAL is the receptor for GDF15 and is required for the anti-obesity effects of the ligand. *Nat. Med.* **23**, 1158–1166.
 41. Lu, J.F., Zhu, M.Q., Xie, B.C., Shi, X.C., Liu, H., Zhang, R.X., Xia, B., and Wu, J.W. (2022). Camptothecin effectively treats obesity in mice through GDF15 induction. *PLoS Biol.* **20**, e3001517.
 42. Day, E.A., Ford, R.J., Smith, B.K., Mohammadi-Shemirani, P., Morrow, M.R., Gutgesell, R.M., Lu, R., Raphenya, A.R., Kabiri, M., McArthur, A.G., et al. (2019). Metformin-induced increases in GDF15 are important for suppressing appetite and promoting weight loss. *Nat. Metab.* **1**, 1202–1208.
 43. Wang, D., Townsend, L.K., DesOrmeaux, G.J., Frangos, S.M., Batchuluun, B., Dumont, L., Kuhre, R.E., Ahmadi, E., Hu, S., Rebalka, I.A., et al. (2023). GDF15 promotes weight loss by enhancing energy expenditure in muscle. *Nature* **619**, 143–150.
 44. Benichou, O., Coskun, T., Gonciarz, M.D., Garhyan, P., Adams, A.C., Du, Y., Dunbar, J.D., Martin, J.A., Mather, K.J., Pickard, R.T., et al. (2023). Discovery, development, and clinical proof of mechanism of LY3463251, a long-acting GDF15 receptor agonist. *Cell Metab.* **35**, 274–286.e10.
 45. Rochette, L., Zeller, M., Cottin, Y., and Vergely, C. (2020). Insights into mechanisms of GDF15 and receptor GFRAL: therapeutic targets. *Trends Endocrinol. Metab.* **31**, 939–951.
 46. Jornayvaz, F.R., Jurczak, M.J., Lee, H.Y., Birkenfeld, A.L., Frederick, D.W., Zhang, D., Zhang, X.M., Samuel, V.T., and Shulman, G.I. (2010). A high-fat, ketogenic diet causes hepatic insulin resistance in mice, despite increasing energy expenditure and preventing weight gain. *Am. J. Physiol. Endocrinol. Metab.* **299**, E808–E815.
 47. Nymo, S., Coutinho, S.R., Jørgensen, J., Rehfeld, J.F., Truby, H., Kulseng, B., and Martins, C. (2017). Timeline of changes in appetite during weight loss with a ketogenic diet. *Int. J. Obes.* **41**, 1224–1231.
 48. Bonacci, G., Baker, P.R.S., Salvatore, S.R., Shores, D., Khoo, N.K.H., Koenitzer, J.R., Vitturi, D.A., Woodcock, S.R., Golin-Bisello, F., Cole, M.P., et al. (2012). Conjugated linoleic acid is a preferential substrate for fatty acid nitration. *J. Biol. Chem.* **287**, 44071–44082.
 49. Charles, R.L., Rudyk, O., Pryszyzna, O., Kamynina, A., Yang, J., Morisseau, C., Hammock, B.D., Freeman, B.A., and Eaton, P. (2014). Protection from hypertension in mice by the Mediterranean diet is mediated by nitro fatty acid inhibition of soluble epoxide hydrolase. *Proc. Natl. Acad. Sci. USA* **111**, 8167–8172.
 50. Fang, W., Xue, H., Chen, X., Chen, K., and Ling, W. (2019). Supplementation with sodium butyrate modulates the composition of the gut microbiota and ameliorates high-fat diet-induced obesity in mice. *J. Nutr.* **149**, 747–754.
 51. Vu, J.P., Luong, L., Parsons, W.F., Oh, S., Sanford, D., Gabalski, A., Lighton, J.R., Piseigna, J.R., and Germano, P.M. (2017). Long-term intake of a high-protein diet affects body phenotype, metabolism, and plasma hormones in mice. *J. Nutr.* **147**, 2243–2251.
 52. Rowan, S., Jiang, S., Chang, M.L., Volkin, J., Cassalman, C., Smith, K.M., Streeter, M.D., Spiegel, D.A., Moreira-Neto, C., Rabbani, N., et al. (2020). A low glycemic diet protects disease-prone Nrf2-deficient mice against age-related macular degeneration. *Free Radic. Biol. Med.* **150**, 75–86.
 53. Li, G., Xie, C., Lu, S., Nichols, R.G., Tian, Y., Li, L., Patel, D., Ma, Y., Brocker, C.N., Yan, T., et al. (2017). Intermittent fasting promotes white adipose browning and decreases obesity by shaping the gut microbiota. *Cell Metab.* **26**, 672–685.e4.
 54. Hatori, M., Vollmers, C., Zarrinpar, A., DiTacchio, L., Bushong, E.A., Gill, S., Leblanc, M., Chaix, A., Joens, M., Fitzpatrick, J.A.J., et al. (2012). Time-restricted feeding without reducing caloric intake prevents metabolic diseases in mice fed a high-fat diet. *Cell Metab.* **15**, 848–860.
 55. Song, P., Zechner, C., Hernandez, G., Cánovas, J., Xie, Y., Sondhi, V., Wagner, M., Stadlbauer, V., Horvath, A., Leber, B., et al. (2018). The hormone FGF21 stimulates water drinking in response to ketogenic diet and alcohol. *Cell Metab.* **27**, 1338–1347.e4.
 56. Bookout, A.L., de Groot, M.H.M., Owen, B.M., Lee, S., Gautron, L., Lawrence, H.L., Ding, X., Elmquist, J.K., Takahashi, J.S., Mangelsdorf, D.J., and Kliewer, S.A. (2013). FGF21 regulates metabolism and circadian behavior by acting on the nervous system. *Nat. Med.* **19**, 1147–1152.
 57. Laeger, T., Henagan, T.M., Albarado, D.C., Redman, L.M., Bray, G.A., Noland, R.C., Münzberg, H., Hutson, S.M., Gettys, T.W., Schwartz, M.W., and Morrison, C.D. (2014). FGF21 is an endocrine signal of protein restriction. *J. Clin. Invest.* **124**, 3913–3922.
 58. Vinales, K.L., Begaye, B., Bogardus, C., Walter, M., Krakoff, J., and Piaggi, P. (2019). FGF21 is a hormonal mediator of the human "thrifty" metabolic phenotype. *Diabetes* **68**, 318–323.

59. Coll, A.P., Chen, M., Taskar, P., Rimmington, D., Patel, S., Tadross, J.A., Cimino, I., Yang, M., Welsh, P., Virtue, S., et al. (2020). GDF15 mediates the effects of metformin on body weight and energy balance. *Nature* 578, 444–448.
60. Mulderrig, L., Garaycoechea, J.I., Tuong, Z.K., Millington, C.L., Dingler, F.A., Ferdinand, J.R., Gaul, L., Tadross, J.A., Arends, M.J., O’Rahilly, S., et al. (2021). Aldehyde-driven transcriptional stress triggers an anorexic DNA damage response. *Nature* 600, 158–163.
61. Ost, M., Igual Gil, C., Coleman, V., Keipert, S., Efstathiou, S., Vidic, V., Weyers, M., and Klaus, S. (2020). Muscle-derived GDF15 drives diurnal anorexia and systemic metabolic remodeling during mitochondrial stress. *EMBO Rep.* 21, e48804.
62. Wang, T., Liu, J., McDonald, C., Lupino, K., Zhai, X., Wilkins, B.J., Hakonarson, H., and Pei, L. (2017). GDF15 is a heart-derived hormone that regulates body growth. *EMBO Mol. Med.* 9, 1150–1164.
63. Gross, B., Pawlak, M., Lefebvre, P., and Staels, B. (2017). PPARs in obesity-induced T2DM, dyslipidaemia and NAFLD. *Nat. Rev. Endocrinol.* 13, 36–49.
64. El Ouarrat, D., Isaac, R., Lee, Y.S., Oh, D.Y., Wollam, J., Lackey, D., Riopel, M., Bandyopadhyay, G., Seo, J.B., Sampath-Kumar, R., and Olefsky, J.M. (2020). TAZ is a negative regulator of PPARgamma activity in adipocytes and TAZ deletion improves insulin sensitivity and glucose tolerance. *Cell Metab* 31, 162–173.e165.
65. Patel, S., Alvarez-Guaita, A., Melvin, A., Rimmington, D., Dattilo, A., Miedzybrodzka, E.L., Cimino, I., Maurin, A.C., Roberts, G.P., Meek, C.L., et al. (2019). GDF15 provides an endocrine signal of nutritional stress in mice and humans. *Cell Metab.* 29, 707–718.e8.
66. Moreno, B., Crujeiras, A.B., Bellido, D., Sajoux, I., and Casanueva, F.F. (2016). Obesity treatment by very low-calorie-ketogenic diet at two years: reduction in visceral fat and on the burden of disease. *Endocrine* 54, 681–690.
67. Barrera, J.G., Sandoval, D.A., D’Alessio, D.A., and Seeley, R.J. (2011). GLP-1 and energy balance: an integrated model of short-term and long-term control. *Nat. Rev. Endocrinol.* 7, 507–516.
68. Luque, R.M., Kineman, R.D., and Tena-Sempere, M. (2007). Regulation of hypothalamic expression of KiSS-1 and GPR54 genes by metabolic factors: analyses using mouse models and a cell line. *Endocrinology* 148, 4601–4611.
69. Katan, M.B. (2009). Weight-loss diets for the prevention and treatment of obesity. *N. Engl. J. Med.* 360, 923–925.
70. Shai, I., Schwarzfuchs, D., Henkin, Y., Shahar, D.R., Witkow, S., Greenberg, I., Golan, R., Fraser, D., Bolotin, A., Vardi, H., et al. (2008). Weight loss with a low-carbohydrate, Mediterranean, or low-fat diet. *N. Engl. J. Med.* 359, 229–241.
71. Hepler, C., Weidemann, B.J., Waldeck, N.J., Marcheva, B., Cedernaes, J., Thorne, A.K., Kobayashi, Y., Nozawa, R., Newman, M.V., Gao, P., et al. (2022). Time-restricted feeding mitigates obesity through adipocyte thermogenesis. *Science* 378, 276–284.
72. Nani, A., Murtaza, B., Sayed Khan, A., Khan, N.A., and Hichami, A. (2021). Antioxidant and anti-inflammatory potential of polyphenols contained in Mediterranean Diet in obesity: molecular mechanisms. *Molecules* 26, 985.
73. Ludwig, D.S. (2002). The glycemic index: physiological mechanisms relating to obesity, diabetes, and cardiovascular disease. *JAMA* 287, 2414–2423.
74. Luukkonen, P.K., Dufour, S., Lyu, K., Zhang, X.M., Hakkarainen, A., Lehtimäki, T.E., Cline, G.W., Petersen, K.F., Shulman, G.I., and Yki-Järvinen, H. (2020). Effect of a ketogenic diet on hepatic steatosis and hepatic mitochondrial metabolism in nonalcoholic fatty liver disease. *Proc. Natl. Acad. Sci. USA* 117, 7347–7354.
75. Wang, D.D., and Hu, F.B. (2018). Precision nutrition for prevention and management of type 2 diabetes. *Lancet Diabetes Endocrinol.* 6, 416–426.
76. Shin, S.Y., Fauman, E.B., Petersen, A.K., Krumsiek, J., Santos, R., Huang, J., Arnold, M., Erte, I., Forgetta, V., Yang, T.P., et al. (2014). An atlas of genetic influences on human blood metabolites. *Nat. Genet.* 46, 543–550.
77. Lee, J., Choi, J., Scafidi, S., and Wolfgang, M.J. (2016). Hepatic fatty acid oxidation restrains systemic catabolism during starvation. *Cell Rep.* 16, 201–212.
78. Zhang, M., Sun, W., Qian, J., and Tang, Y. (2018). Fasting exacerbates hepatic growth differentiation factor 15 to promote fatty acid beta-oxidation and ketogenesis via activating XBP1 signaling in liver. *Redox Biol.* 16, 87–96.
79. Lerner, L., Hayes, T.G., Tao, N., Krieger, B., Feng, B., Wu, Z., Nicoletti, R., Chiu, M.I., Gyuris, J., and Garcia, J.M. (2015). Plasma growth differentiation factor 15 is associated with weight loss and mortality in cancer patients. *J. Cachexia Sarcopenia Muscle* 6, 317–324.
80. Suriben, R., Chen, M., Higbee, J., Oeffinger, J., Ventura, R., Li, B., Mondal, K., Gao, Z., Ayupova, D., Taskar, P., et al. (2020). Antibody-mediated inhibition of GDF15-GFRAL activity reverses cancer cachexia in mice. *Nat. Med.* 26, 1264–1270.
81. Kennedy, A.R., Pissios, P., Otu, H., Roberson, R., Xue, B., Asakura, K., Furukawa, N., Marino, F.E., Liu, F.F., Kahn, B.B., et al. (2007). A high-fat, ketogenic diet induces a unique metabolic state in mice. *Am. J. Physiol. Endocrinol. Metab.* 292, E1724–E1739.
82. Katsumura, S., Siddiqui, N., Goldsmith, M.R., Cheah, J.H., Fujikawa, T., Minegishi, G., Yamagata, A., Yabuki, Y., Kobayashi, K., Shirouzu, M., et al. (2022). Deadenylase-dependent mRNA decay of GDF15 and FGF21 orchestrates food intake and energy expenditure. *Cell Metab.* 34, 564–580.e8.
83. Patel, S., Haider, A., Alvarez-Guaita, A., Bidault, G., El-Sayed Moustafa, J.S., Guiu-Jurado, E., Tadross, J.A., Warner, J., Harrison, J., Virtue, S., et al. (2022). Combined genetic deletion of GDF15 and FGF21 has modest effects on body weight, hepatic steatosis and insulin resistance in high fat fed mice. *Mol. Metab.* 65, 101589.
84. Dubuquoy, L., Rousseaux, C., Thuru, X., Peyrin-Biroulet, L., Romano, O., Chavatte, P., Chamailard, M., and Desreumaux, P. (2006). PPARgamma as a new therapeutic target in inflammatory bowel diseases. *Gut* 55, 1341–1349.
85. Aguilar-Recarte, D., Barroso, E., Zhang, M., Rada, P., Pizarro-Delgado, J., Peña, L., Palomer, X., Valverde, Á.M., Wahli, W., and Vázquez-Carrera, M. (2023). A positive feedback loop between AMPK and GDF15 promotes metformin antidiabetic effects. *Pharmacol. Res.* 187, 106578.
86. Weng, J.H., Koch, P.D., Luan, H.H., Tu, H.C., Shimada, K., Ngan, I., Ventura, R., Jiang, R., and Mitchison, T.J. (2021). Colchicine acts selectively in the liver to induce hepatokines that inhibit myeloid cell activation. *Nat. Metab.* 3, 513–522.
87. Cheng, J.C., Chang, H.M., and Leung, P.C.K. (2011). Wild-type p53 attenuates cancer cell motility by inducing growth differentiation factor-15 expression. *Endocrinology* 152, 2987–2995.
88. Xie, B., Shi, X., Li, Y., Xia, B., Zhou, J., Du, M., Xing, X., Bai, L., Liu, E., Alvarez, F., et al. (2021). Deficiency of ASGR1 in pigs recapitulates reduced risk factor for cardiovascular disease in humans. *PLoS Genet.* 17, e1009891.
89. Xu, M., Li, Y., Wang, X., Zhang, Q., Wang, L., Zhang, X., Cui, W., Han, X., Ma, N., Li, H., et al. (2022). Role of hepatocyte- and macrophage-specific PPARgamma in hepatotoxicity induced by diethylhexyl phthalate in mice. *Environ. Health Perspect.* 130, 17005.
90. Cimino, I., Kim, H., Tung, Y.C.L., Pedersen, K., Rimmington, D., Tadross, J.A., Kohnke, S.N., Neves-Costa, A., Barros, A., Joaquim, S., et al. (2021). Activation of the hypothalamic-pituitary-adrenal axis by exogenous and endogenous GDF15. *Proc. Natl. Acad. Sci. USA* 118, e2106868118.
91. Breen, D.M., Jagarlapudi, S., Patel, A., Zou, C., Joaquim, S., Li, X., Kang, L., Pang, J., Hales, K., Ziso-Qeivanaj, E., et al. (2021). Growth

- differentiation factor 15 neutralization does not impact anorexia or survival in lipopolysaccharide-induced inflammation. *iScience* 24, 102554.
92. Aguilar-Recarte, D., Barroso, E., Gumà, A., Pizarro-Delgado, J., Peña, L., Ruat, M., Palomer, X., Wahli, W., and Vázquez-Carrera, M. (2021). GDF15 mediates the metabolic effects of PPARbeta/delta by activating AMPK. *Cell Rep.* 36, 109501.
 93. Wang, Z., He, L., Li, W., Xu, C., Zhang, J., Wang, D., Dou, K., Zhuang, R., Jin, B., Zhang, W., et al. (2021). GDF15 induces immunosuppression via CD48 on regulatory T cells in hepatocellular carcinoma. *J. Immunother. Cancer* 9, e002787.
 94. Xiong, Y., Walker, K., Min, X., Hale, C., Tran, T., Komorowski, R., Yang, J., Davda, J., Nuanmanee, N., Kemp, D., et al. (2017). Long-acting MIC-1/GDF15 molecules to treat obesity: evidence from mice to monkeys. *Sci. Transl. Med.* 9, eaan8732.
 95. Wu, Y., Li, B., Li, L., Mitchell, S.E., Green, C.L., D'Agostino, G., Wang, G., Wang, L., Li, M., Li, J., et al. (2021). Very-low-protein diets lead to reduced food intake and weight loss, linked to inhibition of hypothalamic mTOR signaling, in mice. *Cell Metab.* 33, 888–904.e6.
 96. Briggs, D.I., Lockie, S.H., Benzler, J., Wu, Q., Stark, R., Reichenbach, A., Hoy, A.J., Lemus, M.B., Coleman, H.A., Parkington, H.C., et al. (2014). Evidence that diet-induced hyperleptinemia, but not hypothalamic gliosis, causes ghrelin resistance in NPY/AgRP neurons of male mice. *Endocrinology* 155, 2411–2422.
 97. Wu, J.W., Wang, S.P., Casavant, S., Moreau, A., Yang, G.S., and Mitchell, G.A. (2012). Fasting energy homeostasis in mice with adipose deficiency of desnutrin/adipose triglyceride lipase. *Endocrinology* 153, 2198–2207.
 98. Lu, J.F., Zhu, M.Q., Zhang, H., Liu, H., Xia, B., Wang, Y.L., Shi, X., Peng, L., and Wu, J.W. (2020). Neohesperidin attenuates obesity by altering the composition of the gut microbiota in high-fat diet-fed mice. *FASEB J* 34, 12053–12071.
 99. Wu, J.W., Wang, S.P., Alvarez, F., Casavant, S., Gauthier, N., Abed, L., Soni, K.G., Yang, G., and Mitchell, G.A. (2011). Deficiency of liver adipose triglyceride lipase in mice causes progressive hepatic steatosis. *Hepatology* 54, 122–132.
 100. Feng, X., Wang, Z., Wang, F., Lu, T., Xu, J., Ma, X., Li, J., He, L., Zhang, W., Li, S., et al. (2019). Dual function of VGLL4 in muscle regeneration. *EMBO J.* 38, e101051.

STAR★METHODS

KEY RESOURCES TABLE

REAGENT or RESOURCE	SOURCE	IDENTIFIER
Antibodies		
Rabbit- <i>anti</i> -ATF4	Proteintech	CAT# 10835-1-AP; RRID: AB_2058600
Rabbit- <i>anti</i> -CHOP	Proteintech	CAT# 15204-1-AP; RRID: AB_2292610
Mouse- <i>anti</i> -GAPDH	Proteintech	CAT# 60004-1-Ig; RRID: AB_2107436
Rabbit- <i>anti</i> -PPAR γ	Cell Signaling Technology	CAT# 2435S; RRID: AB_2166051
GDF15 neutralizing antibody	This paper	N/A
FGF21 antibody	Antibody and Immunoassays Services	N/A
Chemicals, peptides, and recombinant proteins		
Rosiglitazone	Med Chem Express	CAT# HY-17386
recombinant GDF15	R&D	CAT# 8944-GD
AAV8- <i>Scramble</i> -shRNA	Hanbio	N/A
AAV8- <i>Gdf15</i> -shRNA	Hanbio	N/A
AAV8- <i>Pparγ</i> -shRNA	Hanbio	N/A
AAV8- <i>Gdf15</i> -overexpression	Scilia Life Science	N/A
TRIZOL Reagent	Invitrogen	Cat# 15596-026
Novolin R (recombinant human insulin; 100U/mL)	Novo Nordisk	N/A
Critical commercial assays		
Mouse GDF15 ELISA	R&D	CAT# MGD150
Pig GDF15 ELISA	Solarbio	CAT# SEKP-0034
Human GDF15 ELISA	R&D	CAT# DY957
Mouse FGF21 ELISA	R&D	CAT# MF2100
Lipofectamine 3000	Invitrogen	CAT# L3000001
Triglycerides reagent	Jiancheng	CAT# A110-1-1
Dual-luciferase Reporter Assay	Promega	CAT# E1980
Deposited data		
RNA sequencing data	This paper	SRA: PRJNA924349
Source data	This paper	Data S1-Source data
Experimental models: Cell lines		
AML12	ATCC	CAT# CRL-2254; RRID: CVCL_0140
3T3-L1	ATCC	CAT# CL-173; RRID: CVCL_0123
Human primary hepatocyte	Lonza	N/A
Experimental models: Organisms/strains		
C57BL/6J	Huafukang Bioscience	N/A
<i>Gdf15</i> knockout mice	Cyagen	CAT# S-KO-07013
<i>Gfral</i> knockout mice	Cyagen	CAT# S-KO-09987
<i>Pparγ</i> ^{loxP} mice	Jackson Laboratories	Strain#004584; RRID: IMSR_JAX:004584
Bama miniature pig (<i>Sus scrofa</i>)	Chengdu Clonorgan Biotechnology	N/A
Oligonucleotides		
Mouse <i>Gdf15</i> Forward (CTGGCAATGCCTGAACAACG)	This paper	NM_011819.4
Mouse <i>Gdf15</i> Reverse (GGTCGGGACTTGTTCTGAG)		
Mouse β - <i>actin</i> Forward (GACCTGACTGACTACCTCAT)	This paper	NM_007393.5
Mouse β - <i>actin</i> Reverse (CGAAGTCAAGAGCCACATAG)		

(Continued on next page)

Continued

REAGENT or RESOURCE	SOURCE	IDENTIFIER
Mouse <i>Ppara</i> Forward (TACTGCCGTTTTACAAGTGC)	This paper	NM_001113418.1
Mouse <i>Ppara</i> Reverse (AGGTCGTGTTACAGGTAAGA)		
Mouse <i>Pparβ</i> Forward (GCCACAACGCACCCCTTTG)	This paper	NM_001411526.1
Mouse <i>Pparβ</i> Reverse (CCACACCAGGCCCTTCTCT)		
Mouse <i>Pparγ1</i> Forward (AAGAAGCGGTGAACCACTGA)	This paper	NM_001127330.3
Mouse <i>Pparγ1</i> Reverse (GAATGCGAGTGGTCTTCCAT)		
Mouse <i>Pparγ2</i> Forward (TCGCTGATGCACTGCCTATG)	This paper	NM_011146.4
Mouse <i>Pparγ2</i> Reverse (GAGAGGTCCACAGAGCTGATT)		
Mouse <i>Cd36</i> Forward (ATGGGCTGTGATCGGAACCTG)	This paper	XM_001421119.1
Mouse <i>Cd36</i> Reverse (TTTGCCACGTCATCTGGGTTT)		
Mouse <i>Pltp</i> Forward (TGGGACGGTGTGCTCAA)	This paper	NM_011125.3
Mouse <i>Pltp</i> Reverse (CCCACGAGATCATCCACAGA)		
Mouse <i>Cyp4a14</i> Forward (AGCAAAGTGTTCCTCAATGC)	This paper	NM_007822.2
Mouse <i>Cyp4a14</i> Reverse (ACCCCTCTAGATTTGCACCA)		
Mouse <i>Slc27a1</i> Forward (CTGGGACTTCCGTGGACCT)	This paper	NM_011977.4
Mouse <i>Slc27a1</i> Reverse (TCTTGCAGACGATACGCAGA)		
Mouse <i>Me1</i> Forward (CCCTGAGTATGACGCCTTCC)	This paper	NM_001198933.1
Mouse <i>Me1</i> Reverse (GCAACAGACGCTGTTCCCTTG)		
Mouse <i>Scd1</i> Forward (TTCTTGCGATACACTCTGGTGC)	This paper	NM_009127.4
Mouse <i>Scd1</i> Reverse (CGGGATTGAATGTTCTTGTCTG)		
Mouse <i>Cyp8b1</i> Forward (ACAGCGTGATGGAGGAGAGT)	This paper	NM_010012.3
Mouse <i>Cyp8b1</i> Reverse (AGGGGAAGAGAGCCACCTTA)		
Mouse <i>Cyp4a12b</i> Forward (GGGGAGATCAGACCCAAAAGC)	This paper	NM_172306.2
Mouse <i>Cyp4a12b</i> Reverse (ATTCGTGCGGTGCTGAAACCAT)		
Mouse <i>Cpt1b</i> Forward (AAGTGTAGGACCAGCCCCGA)	This paper	NM_009948.2
Mouse <i>Cpt1b</i> Reverse (TGCGGACTCGTTGGTACAGG)		
Mouse <i>Acaa1b</i> Forward (GCGTCCTTAATCACTGGGGT)	This paper	NM_146230.4
Mouse <i>Acaa1b</i> Reverse (CCAGGTGACCCAGCACTACC)		
Mouse <i>Ehhadh</i> Forward (CGGTCAATGCCATCAGTCCAA)	This paper	NM_023737.3
Mouse <i>Ehhadh</i> Reverse (TGCTCCACAGATCACTATGGC)		
Mouse <i>Acox1</i> Forward (GCAGATAAACTCCCCAAGATTCAAGAC)	This paper	NM_001377522.1
Mouse <i>Acox1</i> Reverse (TAAAGTCAAAGGCATCCACCAAAGC)		
Mouse <i>Cyp4a12a</i> Forward (CCTACTATTCTGCCCTTC)	This paper	NM_177406.3
Mouse <i>Cyp4a12a</i> Reverse (TCAGCTCATTATCGCAAAC)		
Pig GDF15 Forward (TCAAGTCCGATAGTCAC)	This paper	NM_001174056.1
Pig GDF15 Reverse (AGTTAAGTTGACGCGAGG)		
Pig PPAR γ Forward (ACTGTCCGTTTCAGAAGTGC)	This paper	NM_214379.1
Pig PPAR γ Reverse (CAGCAGACTCTGGGTTCACT)		
Pig GAPDH Forward (AGGTCCGAGTGAACGGATTTG)	This paper	NM_001206359.1
Pig GAPDH Reverse (ACCATGTAGTGGAGTCAATGAAG)		
Human GDF15 Forward (GCTACGAGGACCTGCTAACC)	This paper	NM_004864.4
Human GDF15 Reverse (ACTTCTGGCGTGAGTATCCG)		
Human β -actin Forward (GAAGAGCTACGAGCTGCCTGA)	This paper	NM_001101.5
Human β -actin Reverse (CAGACAGCACTGTGTTGGCG)		

Software

GraphPad Prism v10.0.0	GraphPad software (Boston, MA)	https://www.graphpad.com
SPSS v.20.0	IBM	N/A

Other

Chow diet	Huafukang Bioscience	CAT# H10010
-----------	----------------------	-------------

(Continued on next page)

Continued

REAGENT or RESOURCE	SOURCE	IDENTIFIER
60% High fat diet	Huafukang Bioscience	CAT# H10060
Ketogenic diet	Xietong Bioscience	CAT# XTKD01
75% High fat diet	Xietong Bioscience	N/A
Oxymax/CLAMS	Columbus Instruments	N/A
Collagen I-coated plates	BD Bioscience	N/A
Hepatocyte basal medium	Lonza	N/A
<i>Gdf15</i> nucleotide probe	Sangon Biotech	N/A

RESOURCE AVAILABILITY

Lead contact

Further information and requests for resources and reagents should be directed to and will be fulfilled by the Lead Contact, Jiang Wei Wu (wujiangwei@nwfufu.edu.cn).

Materials availability

This study did not generate new unique reagents.

Data and code availability

RNA sequencing data is available in the NCBI Sequence Read Archive (SRA) and the accession number is provided in the key resources table. Source data and Western blot images for the figures in the manuscript are available as [Data S1](#). This human trial was registered at chictr.org.cn/indexEN.html under the identifier ChiCTR2300071823: <https://www.chictr.org.cn/showprojEN.html?proj=198176>. No new data code has been generated in this study. Any additional information required to reanalyze the data reported in this paper is available from the [lead contact](#) upon request.

EXPERIMENTAL MODEL AND STUDY PARTICIPANT DETAILS

Human study: Effect of KD on humans

A total of 30 individuals who met all the following eligibility criteria were recruited in the First Affiliated Hospital of the Air Force Medical University (Ethical approval KY20232166-C-1). Inclusion criteria were: (i) ethnic Chinese; (ii) medication-free, non-smokers without any history of neurological, gastrointestinal or eating disorders; (iii) alcohol consumption <10 g/d for women and <20 g/d for men; (iv) overweight (BMI ≥ 28 and <30 kg/m²) or obesity (BMI 30–36 kg/m²); (v) without diabetes mellitus; (vi) aged 18–60 years old. Exclusion criteria were: (i) intolerance to KD diet; (ii) sickness and use of medication; (iii) pregnancy. This trial was registered at chictr.org.cn/indexEN.html under the identifier ChiCTR2300071823: <https://www.chictr.org.cn/showprojEN.html?proj=198176>.

All participants provided written informed consent before taking part in the study.

A schematic diagram for KD dietary intervention is shown in [Figure 1J](#). Participants were under KD diet (~1800 kcal energy per day, ~6% as carbohydrate, ~72% as fat, and 22% as protein) for 14 days. Among the 30 participants, nineteen of them (13 male and 6 female, the mean \pm SD age and BMI were 36.2 \pm 6.9 years and 31.67 \pm 2.33 kg/m² respectively) completed the 14-day KD dietary intervention. The other eleven participants dropped out of the trial due to reported consumption of carbohydrate-rich diet, infection with COVID and application of medication for symptom relief, as well as time and scheduling conflicts. Data were compared at the end of the study to the baseline by paired Student's *t* test. No data were excluded from analysis."

Animal studies

All the experimental procedures were followed the Guide for the Care and Use of Laboratory Animals (Eighth Edition, ISBN-10: 0-309-15396-4). Animal studies were approved by the ethics committee of the Northwest A&F University (Permission ID: 20191205-008). Bama miniature pigs were purchased from Chengdu Clonorgan Biotechnology Co. LTD and were raised as we previously described.⁸⁸ Briefly, pigs had free access to food and water and maintained at stable room temperature (20 \pm 2°C). C57BL/6J mice were purchased from the Beijing Huafukang Bioscience (Beijing, China). *Gdf15*^{-/-} mice and *Gfra1*^{-/-} mice were purchased from Cyagen Biosciences (Guangzhou, China). Hepatocyte-specific *Ppar γ* knockout mice with C57BL/6J background (*Ppar γ* ^{Δ Hep}) and the littermate control (*Ppar γ* ^{flox/flox}) mice were acquired as described previously.⁸⁹ Mice were housed in a controlled environment (12-h light/dark cycle, light cycle from 7 a.m. to 7 p.m., and dark cycle from 7 p.m. to 7 a.m.) and were maintained at stable room temperature (23 \pm 2°C) with free access to food and water. Animals were randomly divided into different groups as specified. The classic KD (Jiangsu Xietong Pharmaceutical Bio-engineering, Nanjing, China) was used for mice dietary intervention. Its composition was listed in [Table S1](#). Unless otherwise specified, male C57BL/6J mice were fed 60% HFD (H10060, Beijing Huafukang Bioscience) to induce obesity. The body weight of individual mouse was shown in [Table S2](#).

METHOD DETAILS

Pig study: Effect of KD on pigs

Obese Bama miniature pigs were induced by high sugar and fat diet (HSFD) (containing 33% sugar and 10% lard, purchased from Chengdu Hualanxu Biotechnology, Chengdu, China) for 12 weeks and then randomly assigned for control (HSFD) or KD (containing 77% lard) for 15 days (6 pigs per group). On the day of first dietary intervention, body weight of study groups (mean \pm SEM) was 38.22 ± 1.15 vs. 38.55 ± 0.78 kg for control diet and KD feedings, respectively. On day 15, pigs were weighed and plasma samples were carefully collected before sacrificed.

Mouse study 1 (MS1): Effect of KD on mice

Eight-week-old male C57BL6/J mice fed HFD for 12 weeks were used (body weight, mean \pm SEM, 39.11 ± 0.35 g). Mice were then randomly assigned for HFD or KD intervention (6 mice per group) for 15 days. Body weight and energy intake were monitored every 3 days. On day 15, mice were anesthetized in chambers saturated with isoflurane after 6 h starvation and then sacrificed by cardiac puncture. After centrifugation at 6,000 rpm at 4°C for 5 min, plasma samples were separated. Organs and tissues were carefully collected, weighed, and frozen at -80°C until subsequent analysis.

Mouse study 2 (MS2): HFD and KD, *Gdf15*^{-/-} mice

Experimental cohorts of male *Gdf15*^{-/-} and *Gdf15*^{+/+} mice were obtained by het x het breeding pairs. On the day of first dietary intervention, body weight of study groups (mean \pm SEM) was 32.17 ± 0.64 g versus 32.15 ± 0.70 g for *Gdf15*^{+/+} HFD and KD feedings, respectively, and 32.16 ± 0.97 g versus 32.19 ± 0.93 g for *Gdf15*^{-/-} HFD and KD feedings, respectively. Mice were received HFD or KD for 30 days, and their body weight and energy intake were monitored every 3 days. On day 30, mice were euthanized by terminal anesthesia, and plasma was carefully obtained. Tissues were fresh frozen and kept at -80°C until subsequent analysis.

Mouse study 3 (MS3): HFD and KD, *Gfrah1*^{-/-} mice

Experimental cohorts of male *Gfrah1*^{-/-} and *Gfrah1*^{+/+} mice were obtained by het x het breeding pairs. On the day of first dietary intervention, body weight of study groups (mean \pm SEM) was 32.83 ± 0.75 g versus 32.73 ± 0.48 g for *Gfrah1*^{+/+} HFD and KD feedings, respectively, and 33.00 ± 0.58 g versus 32.91 ± 0.86 g for *Gfrah1*^{-/-} HFD and KD feedings, respectively. Mice were received HFD or KD for 30 days, and their body weight and energy intake were monitored every 3 days. On day 30, mice were euthanized by terminal anesthesia, and plasma was carefully obtained. Tissues were fresh frozen and kept at -80°C until subsequent analysis.

Mouse study 4 (MS4): AAV8-mediated *Gdf15* knockdown

To knock down *Gdf15* in the liver, we transduced AAV8 shRNA against *Gdf15* (designed and synthesized by Hanbio, Shanghai, China) into mice. Scramble shRNA was used as a negative control. Target sequences are listed in [key resources table](#). A schematic diagram for mice administration is shown in [Figure 4C](#). In brief, male C57BL6/J mice aged 8 weeks were switched from standard chow to 60% HFD for 8–10 weeks. Mice were then randomly divided into four groups: AAV8-Scramble + HFD, AAV8-Scramble + KD, AAV8-*Gdf15* + HFD, and AAV8-*Gdf15* + KD. AAV was diluted in saline to 1×10^{12} vector genomes/ml, and 100 μL was injected through the tail vein for each mouse. Body weight and energy intake were measured every 3 days. On the day of 21 after AAV injection, body weight of study groups (mean \pm SEM) was 36.82 ± 0.75 g (AAV8-Scramble + HFD), 36.79 ± 0.52 g (AAV8-Scramble + KD), 36.74 ± 0.77 g (AAV8-*Gdf15* + HFD), and 36.83 ± 0.26 g (AAV8-*Gdf15* + KD). Then mice started to receive HFD or KD for 27 days. The plasma was obtained as in *Mouse study 1*.

Mouse study 5 (MS5): AAV8-mediated *Ppar γ* knockdown

To knock down *Ppar γ* expression in the liver, we transduced AAV8 system carrying shRNA against *Ppar γ* (designed and synthesized by Hanbio, Shanghai, China) into mice, and scramble shRNA was used as a negative control. Target sequences are listed in [key resources table](#). A schematic diagram for mice administration is shown in [Figure 6A](#). In brief, C57BL/6 mice aged 7–8 weeks were switched from standard chow to 60% HFD for 7–8 weeks. Mice were then randomly divided into four groups: AAV8-Scramble + HFD, AAV8-Scramble + KD, AAV8-*Ppar γ* + HFD, and AAV8-*Ppar γ* + KD. AAV was diluted in saline to 1×10^{12} vector genomes ml^{-1} , and 100 μL was injected through the tail vein for each mouse. Body weight and energy intake were measured every 3 days. Twenty-one days after AAV injection, body weight of study groups (mean \pm SEM) was 36.04 ± 0.76 g (AAV8-Scramble + HFD), 36.02 ± 0.52 g (AAV8-Scramble + KD), 35.96 ± 0.77 g (AAV8-*Ppar γ* + HFD), and 36.05 ± 0.26 g (AAV8-*Ppar γ* + KD). Mice then started to receive HFD or KD for 21 days. Finally, mice were sacrificed and plasma was obtained as in *Mouse study 1*.

Mouse study 6 (MS6): *Ppar γ* ^{Δ^{Hep}} mice

We used cre x *loxP* system to create *Ppar γ* hepatocyte specific knockout mice (*Ppar γ* ^{Δ^{Hep}}). A schematic diagram for mice administration is shown in [Figure 6E](#). On the first day of diet feeding, body weight of study groups (mean \pm SEM) was 36.04 ± 0.76 g versus 36.02 ± 0.52 g for *Ppar γ* ^{*fl/fl*} HFD and KD feedings, respectively, and 35.96 ± 0.77 g versus 36.05 ± 0.26 g for *Ppar γ* ^{Δ^{Hep}} HFD and KD feedings, respectively. Mice were received HFD or KD for 21 days, and their body weight and energy intake were monitored every 3 days. On day 21, mice were euthanized by terminal anesthesia and plasma was obtained as in *Mouse study 1*. Tissues were fresh frozen and kept at -80°C until subsequent analysis.

Mouse study 7 (MS7): *Ppar $\gamma^{\Delta\text{Hep}}$* mice with GDF15 overexpression

A schematic diagram for mice administration is shown in Figure 7A. Mice (*Ppar $\gamma^{\text{fl/fl}}$* and *Ppar $\gamma^{\Delta\text{Hep}}$*) were transduced AAV8 system carrying shRNA overexpressing GDF15 (designed and synthesized by Scilia Life Science, Beijing, China) once via tail vein injection, scramble shRNA was used as a negative control. Target sequences are listed in key resources table. AAV was diluted in saline to 1×10^{12} vector genomes ml^{-1} , and 100 μL was injected for each mouse. Body weight and energy intake were measured every 3 days. On day 14 after AAV injection, body weight of study groups (mean \pm SEM) was 37.00 ± 0.73 g for *Ppar $\gamma^{\text{fl/fl}}$* mice receiving AAV8 Scramble, and 36.66 ± 0.77 g versus 36.98 ± 0.21 g for *Ppar $\gamma^{\Delta\text{Hep}}$* mice receiving AAV8 Scramble and AAV8 *Gdf15* overexpression, respectively. Fourteen days after AAV injection, mice started to receive KD for 21 days. Finally, mice were sacrificed and plasma was carefully obtained.

Mouse study 8 (MS8): *Ppar $\gamma^{\Delta\text{Hep}}$* mice with recombinant GDF15 administration

A schematic diagram for mice administration is shown in Figure 7H. In brief, mice (weighted about 36 g) were treated with vehicle or recombinant GDF15 (0.1 mg kg^{-1} , subcutaneous injection). This dose is chosen based on previous studies^{39,65,90} every other day for 21 days with KD feeding. Their body weight and energy intake were monitored every 3 days.

Mouse study 9 (MS9): Effects of different diets on plasma levels of GDF15

Male C57BL6/J mice aged 8 weeks were switched from standard chow to 60% HFD for 13 weeks and then randomly assigned for the experiments. For Mediterranean diet feeding, mice were orally administrated with conjugated linoleic acid and sodium nitrite in 200 μL PEG 400 for 7 days as described.^{48,49} A low-fat diet (20% protein, 70% carbohydrate, 10% fat), high protein diet (60% protein, 30% carbohydrate, 10% fat), and low glycemic index diet (low glycemic starch was composed of 70% amylose/30% amylopectin) were given to mice for 7 days as described.^{50–52}

Mouse study 10 (MS10): Effects of different fasting regimes on plasma levels of GDF15

Male C57BL6/J mice aged 8–9 weeks were switched from standard chow to 60% HFD for 14 weeks. Intermittent fasting (mice had free access to food for 24 h, followed by a 24-h fast for 3 cycles) and time-restricted feeding (mice had access to food during natural nocturnal feeding time for 7 days) were carried out in mice as described.^{53,54} At the end of dietary intervention, plasma was obtained from fasting mice as in *Mouse study 1*.

Mouse study 11 (MS11): GDF15 antibody validation

Three-month-old C57BL/6 mice were treated with either vehicle or recombinant GDF15 (0.1 mg kg^{-1}). On day 7, GDF15-treated mice were divided into two groups, receiving either GDF15 antibody (5.5 mg kg^{-1} , subcutaneous injection, every other day, the dose was selected based on previous reports on the efficiency of GDF15 neutralizing antibody^{91,92}) or IgG control (subcutaneous injection, every other day) for 5 days. Generation of GDF15 neutralizing antibody was acquired as described.⁹³

Mouse study 12 (MS12): GDF15 antibody neutralization in mice

GDF15 antibody neutralization was performed as previously described with minor modifications.^{41,94} Briefly, one week before study start, mice were randomly assigned for the experiments. On the day of first dietary intervention, body weight of study groups (mean \pm SEM) was 44.94 ± 0.75 g versus 45.23 ± 0.87 g for HFD + IgG and KD + IgG feedings, respectively, and 44.68 ± 0.91 g versus 44.84 ± 0.68 g for HFD + Anti-GDF15 and KD + Anti-GDF15, respectively. Mice were treated with either GDF15 neutralizing antibodies (5.5 mg kg^{-1} body weight, every other day) or IgG control through subcutaneous injection for a duration of 30 days. Body weight and energy intake were monitored every 3 days.

Mouse study 13 (MS13): Pair feeding experiment

Pair feeding test was performed as described.^{95,96} In brief, we divided mice into three groups: (1) HFD *ad libitum* fed, (2) KD *ad libitum* fed, and (3) HFD pair-fed to match the calories consumed by the corresponding KD-fed group the day before. Mice were housed individually. On the day of first dietary intervention, body weight of study groups (mean \pm SEM) was 39.13 ± 0.64 g (*Ad libitum* HFD), 38.77 ± 0.33 g (*Ad libitum* KD), and 38.90 ± 0.71 g (Pair-fed HFD). Mice were fed HFD or KD for 9 days. Their body weight and energy intake were measured daily.

Mouse study 14 (MS14): *Gdf15 $^{-/-}$* mice with FGF21 antibody neutralization

Mice (*Gdf15 $^{-/-}$* and *Gdf15 $^{+/+}$* mice) aged 8 weeks were switched from standard chow to 60% HFD for 8 weeks, and then randomly assigned for HFD or KD for 30 days. On the day of first dietary intervention, body weight of study groups (mean \pm SEM) was 36.48 ± 0.30 g (*Gdf15 $^{+/+}$* + HFD + IgG), 36.70 ± 0.77 g (*Gdf15 $^{+/+}$* + KD + Anti-FGF21), 36.28 ± 0.86 g (*Gdf15 $^{-/-}$* + HFD + IgG), and 36.47 ± 0.50 g (*Gdf15 $^{-/-}$* + KD + Anti-FGF21). A schematic diagram for mice administration is shown in Figure S4C. On day 12, mice were treated with either FGF21 neutralizing antibodies (100 $\mu\text{g kg}^{-1}$ body weight) or IgG control (tail vein, every three days) until the end of the duration. Body weight and energy intake were monitored every 3 days.

Plasma analysis

The plasma biochemical parameters include ALT, AST, TG were measured using an automatic biochemical analyzer (Hitachi 7180, Tokyo, Japan) in the Yangling Demonstration Zone Hospital. Levels of GDF15 were measured using GDF15 enzyme-linked immunosorbent assay (MGD150, R&D, Minneapolis, USA for mice; SEKP-0034, Beijing Solarbio Science & Technology, Beijing, China for pigs; DY957, R&D, Minneapolis, USA for humans). Levels of FGF21 was measured using enzyme-linked immunosorbent assay kit (MF2100, R&D, Minneapolis, USA).

Liver TG analysis

The TG of liver tissues was measured using a TG quantification kit (Jiancheng, Nanjing, Jiangsu, China) according to the manufacturer's instructions.

Calorimetry

This was determined by using Oxymax/CLAMS as described.⁹⁷ Briefly, mice were placed in individual metabolic cages and allowed to acclimate for a period of 48 h before data collection. Energy expenditure was measured with an Oxymax/Comprehensive Lab Animal Monitoring System (Columbus Instruments, Columbus, OH). Measurements were performed for the dark (from 18:00 to 06:00) or light (from 06:00 to 18:00) period under *ad libitum* feeding conditions.

Real-time qPCR and Western blots

Total RNAs were extracted from tissue or cultured cells using TRIzol reagent. The cDNA synthesis and qPCR assay were performed as previously described.⁹⁸ The relative mRNA levels were calculated by the $2^{-\Delta\Delta Ct}$ method. The sequence of primers used were listed in [key resources table](#). Western blots were performed as described.⁹⁹

In situ hybridization

Liver, ileum, and colon were collected for *in situ* hybridization. Tissues were dissected and placed into 10% formalin/PBS for 24 h at room temperature, transferred to 70% ethanol, and processed into paraffin. *In situ* hybridization was performed to detect GDF15 expression in tissue specimens using a nucleotide probe. The GDF15 probe was designed and synthesized by Sangon Biotech (Shanghai, China): 5'-CUUCAAGAGUUGCCUGCACAGUCUCCAAGUG-3', 5' labeled with Cy3-dUTP tag. Hybridization specificity was confirmed by the absence of staining in *Gdf15*^{-/-} mice.

GTT and ITT

For GTT, 6h-fasted mice were received an intraperitoneal injection of glucose (2 g kg⁻¹ body weight). For ITT, overnight-fasted mice were received an intraperitoneal injection of insulin (Humulin R, Eli Lilly, Indianapolis, USA) (1 units kg⁻¹ body weight). Tail blood glucose levels were measured at indicated points (0, 30, 60, 90, and 120 min) after injection.

RNA-sequencing and bioinformatic analyses

For transcriptome sequencing, total RNA was extracted from liver samples by TRIzol (Invitrogen) following the standard protocol. The library preparation, sample clustering, and sequencing were described previously. Briefly, the NEBNext Ultra RNA Library Prep Kit for Illumina (NEB) was used to generate the sequencing library, the TruSeq PE Cluster Kit v3-cBot-HS (Illumina) was used to do sample clustering, and the sequencing was carried out on the Illumina NovaSeq 6000 platform.

Cell culture

AML12 cell lines, 3T3-L1 cell lines were obtained from the American Type Culture Collection (ATCC) and were maintained in DMEM: F12 (SH30022.01, HyClone, CT, USA) supplemented to a final concentration of 10% fetal calf bovine plasma (FBS) (Z7186FBS-500, ZETA LIFE, CA, USA) and antibiotics at 37°C under an atmosphere of 95% air and 5% CO₂. After 48 h, 3T3-L1 cells were differentiated by exposure to 3-isobutyl-1-methylxanthine (0.5 mmol/L), dexamethasone (1 μmol/L), insulin (10 μg/mL), and 10% FBS. Rosiglitazone (Med Chem Express, HY-17386, Shanghai, China) was added for 24h and the medium was carefully collected and stored at -80°C for further analysis. Primary human hepatocyte cultures were purchased from Lonza (Walkersville, MD) and cultured in collagen I-coated plates (BD Bioscience, Bedford, MA) with hepatocyte basal medium supplemented with HCM SingleQuots growth factors (Lonza, Walkersville, MD).

Plasmids

In order to construct a plasmid encoding HA-PPAR_γ, the HA-tag was added at the N-terminus of PPAR_γ. The WT-PPAR_γ was cloned into the BamHI and XhoI sites of the pcDNA3.1-HA vector.

Plasmid transfection and luciferase reporter assay

The plasmids were transfected into AML12 cells using Lipofectamine 3000 (L3000001, Invitrogen, California, USA). The relative luciferase activity was measured using the Dual-luciferase Reporter Assay System (E1980, Promega, Wisconsin, USA) following the manufacturer's instructions.

Chromatin immunoprecipitation (ChIP) qPCR

ChIP qPCR were performed as described.¹⁰⁰ Antibodies against mouse IgG (Santa Cruz, sc-2025) and PPAR γ (2435S, CST) were applied. The DNA immunoprecipitated by the antibodies was detected by RT-qPCR. The primers used are listed in [key resources table](#).

QUANTIFICATION AND STATISTICAL ANALYSIS

Values are presented as mean \pm SEM. Statistical comparisons for two groups were performed by the Student's *t* test and for more than two groups, by ordinary 1-way ANOVA followed by Tukey's multiple comparison testing with GraphPad Prism 9 software (GraphPad Software, La Jolla, CA, USA), **p* < 0.05; ***p* < 0.01; ****p* < 0.001.